SAI-79-014-CP/R

PRELIMINARY REPORT: IMPROVEMENT OF A MATHEMATICAL MODEL OF A LARGE OPEN FIRE

P. T. Harsha, W. N. Bragg and R. B. Edelman

Science Applications, Inc.
Combustion Dynamics and Propulsion
Technology Division
21133 Victory Blvd., Suite 216
Canoga Park, California 91303

Prepared for

National Aeronautics and Space Administration
Ames Research Center
Moffett Field, California 94035

Contract No. NAS2 - 10327

September 1979

TABLE OF CONTENTS

LIST OF FIGURES

LIST OF FIGURES (continued)

I. INTRODUCTION

Because of the high-strength for light weight capability of fiber/epoxy structural materials, a significant increase in their use in commercial aircraft structures has been stimulated by the positive effect on fuel conservation that such structures would involve. However, massive utilization of new materials must be preceded by a thorough examination of any potential hazard created by their use. In the case of carbon fiber materials, a potential hazard connected with the release of the fibers into the atmosphere in an aircraft accident resulting in fire has been identified, and is being evaluated.

A necessary part of the hazard evaluation is the determination of the detailed characteristics of large liquid fuel fires, including the spatial variation in flame velocity, temperature, soot concentration, etc., and the manner in which carbon fibers released in lower regions of a large fire are transported and consumed (oxidized) within the fire. To provide the necessary detailed prediction of the characteristics of these fires, a mathematical model was developed by SAI, as reported in Ref. 1. The model includes a characterization of the transport and consumption of carbon fibers in the fire, coupled to a solution of the mass, momentum, and energy transport equations for the gas phase, and a model for the gas phase chemistry involved in hydrocarbon fuel combustion.

During the course of the development of the analysis, a number of assumptions were made in the modeling of the physical phenomena involved in large pool fires. In large part these assumptions were made necessary by the paucity of available experimental data on such fires.

As the work progressed, it became apparent that uncertainties in the analytic predictions of fire characteristics and particularly fiber transport and consumption were somewhat larger than was acceptable for the application. These uncertainties were a consequence, for example, of the uncertainties in the rate that air being entrained into a fire mixes with fuel vapor, in the quantity of soot produced, and in the consumption rate for carbon fibers. To improve the accuracy of the predictions, and therefore of the overall assessment of the hazards resulting from a fire involving carbon composite materials, an experimental program was initiated, sponsored by NASA-Langley, designed and managed by NASA-Ames, and carried out at the NASA White Sands Test Facility. In this program, detailed temperature and concentration measurements are being obtained for JP-4 pool fires, with fuel pool diameters of 7.62 meters (25 feet), 15.24 meters (50 feet) and 30.48 meters (100 feet). An instrumentation array involving measurements of temperature and composition along radii of the fire at heights of 0.72 meters (2.35 feet), 1.43 meters (4.7 feet),2.37 meters (9.4 feet),5.73 meters (18.8 feet),11.4 meters (37.5 feet), and 22.8 meters (70.0 feet) was laid out, based on the results of the initial pool fire structure characterization obtained from calculations made using the model described in Reference 1.

While the data obtained in the pool fire test program are in good qualitative agreement with the results of the pool fire calculations, some quantitative disagreement exists, as was expected. In this report, the results of a preliminary study of model modifications which improve the agreement of the calculations with the available data are described. Because of the short duration of the effort described in this report, modifications were concentrated in three major areas: the turbulence model, the characterization of the consumption rate for carbon fibers, and the characterization of the gas-phase chemistry. Furthermore, the modifications were carried out using data obtained from the

two 50-foot fire tests performed at White Sands for comparison, since these data were the best available during the course of the present work. A more thorough comparison, involving additional data, as well as further model modifications, will be carried out and reported in subsequent work.

In this preliminary report, the overall pool fire model will be outlined in general. This outline is followed by a description of the modifications made to the initial model to enhance the quantitative agreement between the predictions and experimental data. Results of calculations using the modified model are then shown in comparison with the data for the 50-foot fire. This is followed by a presentation of carbon fiber flux and consumption predictions for fire sizes of 7.6 meters (25 feet), 10.7 meters (35 feet) and 15.2 meters (50 feet) diameter.

2. INITIAL FIRE MODEL DESCRIPTION

Modeling of the physical processes occuring in a pool fire with the presence of carbon fiber particles involves consideration of a number of basic physical mechanisms including diffusion, inertia, viscosity, chemistry, chemical kinetics, gravity, turbulent transport, and the transport of particulate material. If we restrict our attention to the axisymmetric fire problem, with specified rates of fuel vaporization, the computation becomes one of an axisymmetric, buoyant, two phase, chemically reacting, turbulent flow.

The technique used for the solution of the fire flow field is that reported by Boccio, Weilerstein, and Edelman (Ref. 2). This technique provides a numerical solution for the equations describing the transport of mass, momentum, energy, and chemical and particulate species in a two-phase reacting flowfield, including the interchange terms representing mass, momentum, and energy transfer between the gas and particulate phases. The particulates (soot, carbon fibers, and carbon fiber clusters) are divided into ten classes based on particle size, and each class is treated as a particulate species; thus in addition to gas phase species transport equations there are ten particulate-phase species transport equations involved in the solution. These equations, and the assumptions embodied in them, are described in detail in Ref. 2.

The physical models required for the fire flowfield solution include models for turbulent transport of momentum, energy, and species; a model for the chemistry occuring in the gas phase, a model for the consumption of particulate species, and a model for the thermal radiation from the fire to its surroundings. The basic models for these mechanisms used in the initial fire model (Ref. 1) were as follows:

Turbulent transport was modeled using an eddy viscosity to obtain the turbulent shear stress. This eddy viscosity was taken to be a constant within the fire in the initial modeling effort. As is described below, in the model modification work outlined in this report, a spatially varying eddy viscosity model has been adopted. The eddy viscosity model defines

the transport of momentum; through the specification of Prandtl and Schmidt numbers diffusivities for heat and mass are also defined, as is described in more detail in Ref. 1.

Gas phase chemistry was modeled in the work described in Ref. 1 using a complete-combustion hydrocarbon chemistry formulation, in which the local fuel and air at each radial location in the plume were assumed to react with each other instantaneously upon coming in contact due to mixing. The products of combustion were defined by the local fuel-air ratio and temperature, with provision for the formation of soot in certain regions of the fire. Such complete-combustion models have been shown (Ref. 2) to adequately model the effects of gas-phase heat release in certain reacting fire plumes. However, the experimental results for large JP-4 pool fires obtained at the White Sands facility indicated that considerable unmixedness effects exist in these large pool fires, and in the present work a simple unmixedness model was adopted for the gas phase chemistry computation.

Particulate species consumption was modeled using the rate obtained by Lee, Thring, and Beer (Ref. 3) for the consumption of carbon particles. As noted earlier, the present formulation includes up to ten particle classes, defined by average particle size. The particulate consumption rate expression is a function of the particle size, and thus is applied to each of the particle classes in the solution. Provision was also made to compute particulate transport in the fire without particle consumption. Recent data obtained at NASA-Langley indicate that carbon fiber consumption rates may be higher than that predicted using the basic Lee, Thring and Beer model, and in the present work this model was modified to provide better agreement with the available carbon fiber consumption data.

Thermal radiation was modeled through the assumption that the particulate species are the primary radiating species and that the radiation can be accounted for using an optically thin limit approximation.

3. EXPERIMENTAL RESULTS

Data from three experiments involving two fire sizes were available for comparison with model predictions during this preliminary effort. These data included two sets of measurements for the 15.24 meter (50 foot) fire and one set for a 7.62 meter (25 foot) fire. All tests were run in essentially zero wind conditions.

Full details of the test facility layout, instrumention used, and results of all of the pool fire tests carried out at the NASA White Sands Test Facility will be described in a forthcoming data report. A selection of these results is, however, included in this section to provide the background for the model modification effort.

The primary data utilized in the model modification effort were obtained in the two 15.24 meter (50 foot) diameter fire tests. Radial temperature profiles from these tests are shown in Figures 1-5, at heights above ground of 1.43 meters (4.7 feet), Figure 1, 2.87M (9.4 feet), Figure 2, 5.73M (18.8 feet), Figure 3, 11.43M (37.5 feet), Figure 4, and 21.34M (70 feet), Figure 5. During the tests, thermocouple readings at each measurement location were sampled at 1 second intervals, resulting in a detailed temperature-time history at each location. To produce the results shown on these figures, the data were smoothed using two averaging techniques. First, the detailed measurements were smoothed using a five-second running average technique; that is, the measurement associated with a given time is the average of the measurement made at that time and the preceding four measurements at one-second time intervals. The thermocouple temperature-time history produced using this smoothing technique was then examined to locate a region, generally spanning 60-90 seconds duration within the first two minutes of the fire test, over which the flame had maintained a reasonably steady spatial location, and the five-second running average data obtained during this time period were then again averaged over the steady-state time period, to obtain an overall average compatible with the steady-state fire model assumptions. Figures 1-5 depict these averaged points with symbols given on the figure legends; also shown are the maximum and minimum

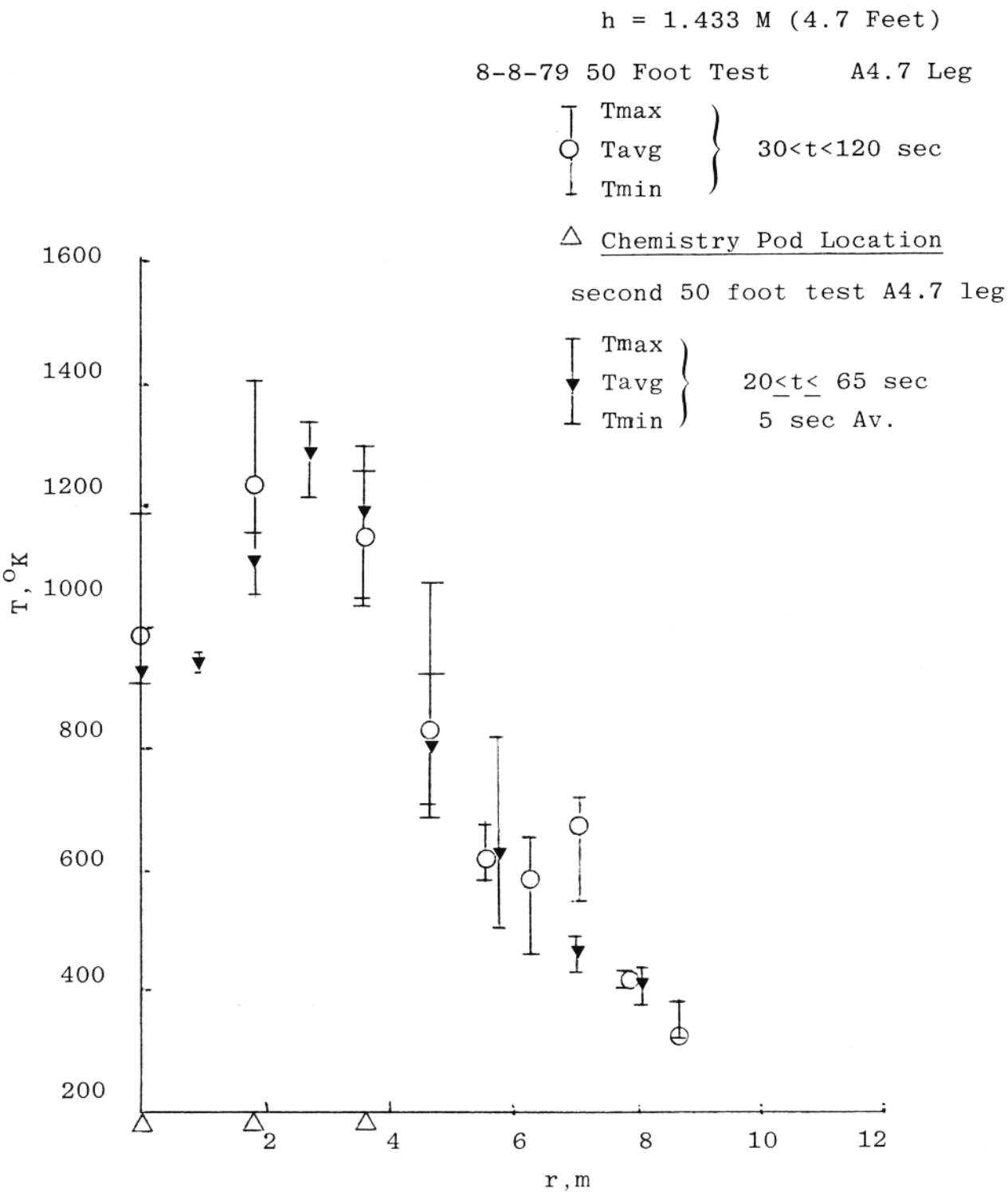

Figure 1. Experimental Radial Temperature Profiles, 15.24 M (50 Foot) Fire Test, Height = 1.433 M (4.7 Feet).

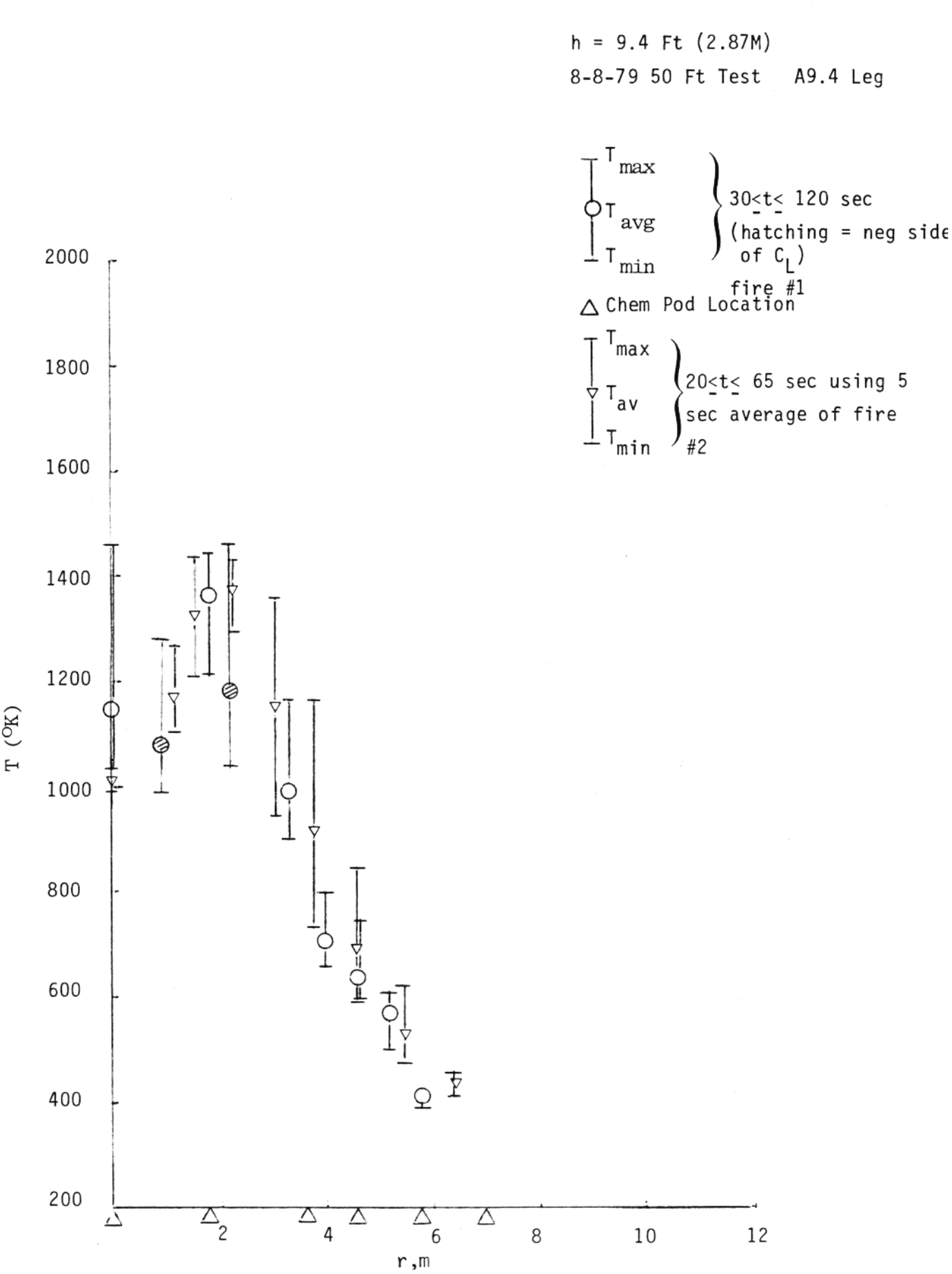

Figure 2. Experimental Radial Temperature Profiles, 15.24M (50 Foot) Fire Test, Height = 2.87M (9.4 Ft)

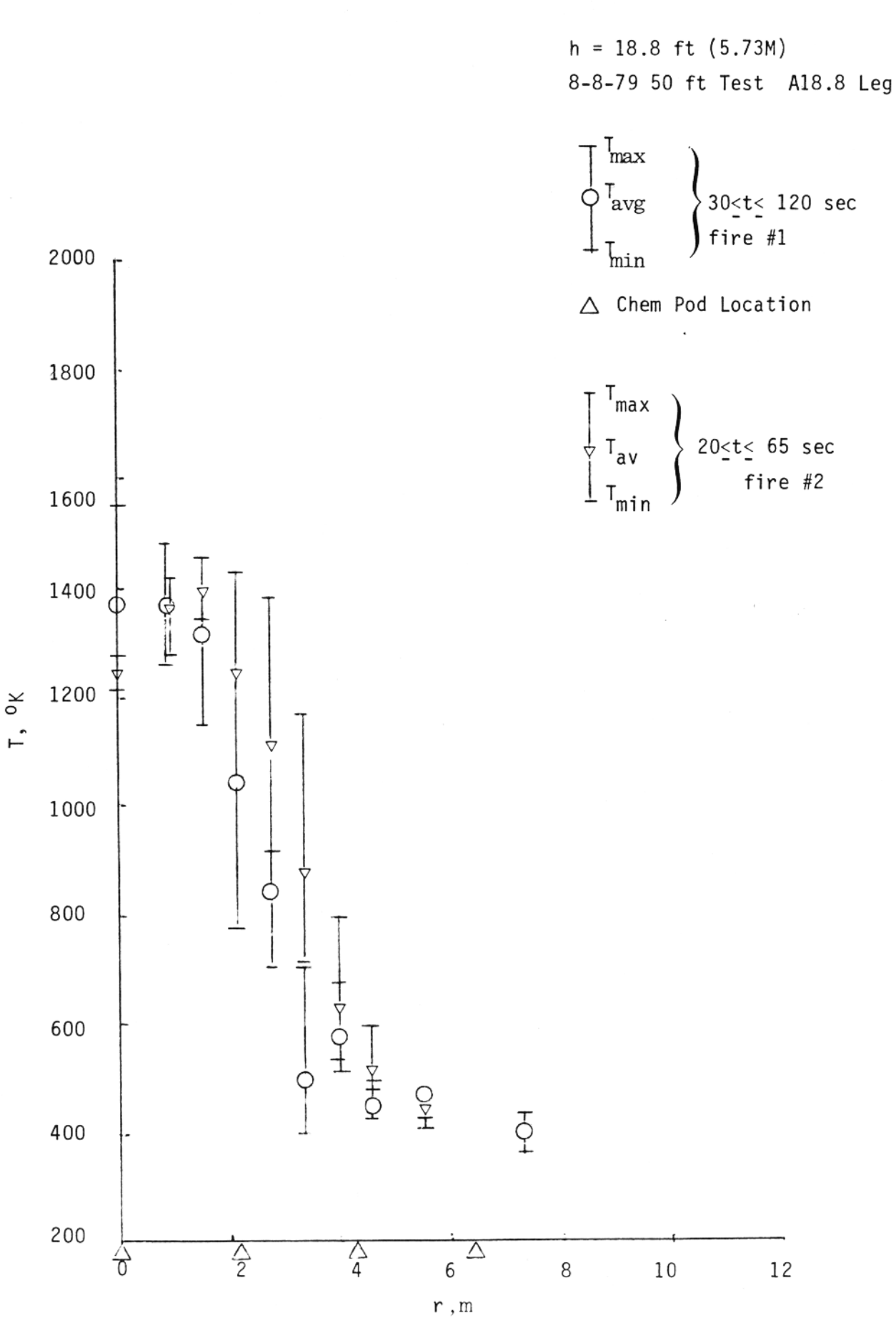

Figure 3. Experimental Radial Temperature Profiles, 15.24M (50 Foot) Fire Test, Height = 5.73M (18.8Ft)

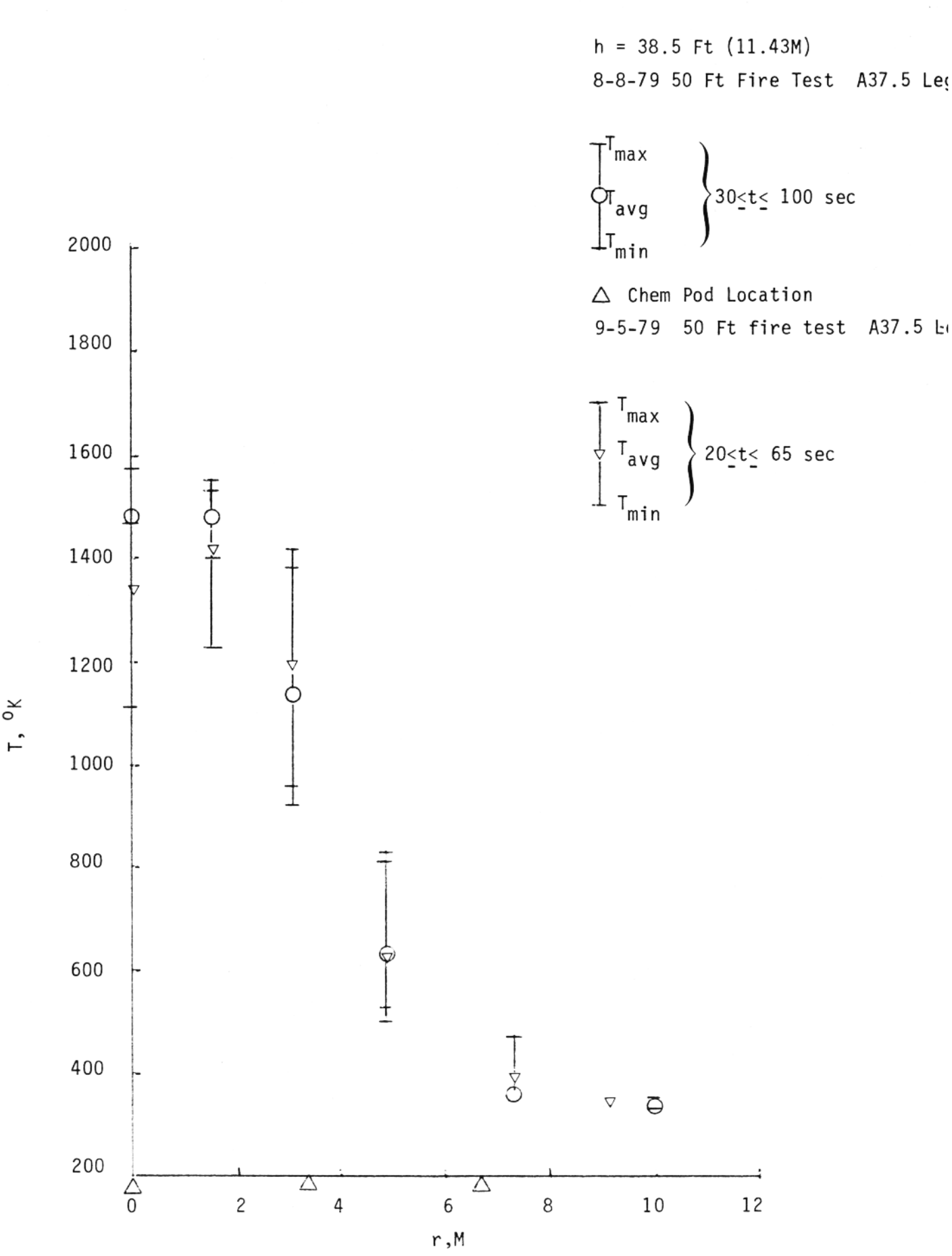

Figure 4. Experimental Radial Temperature Profiles, 15.24M (50 Foot) Fire Test, Height = 11.43M (37.5 Ft)

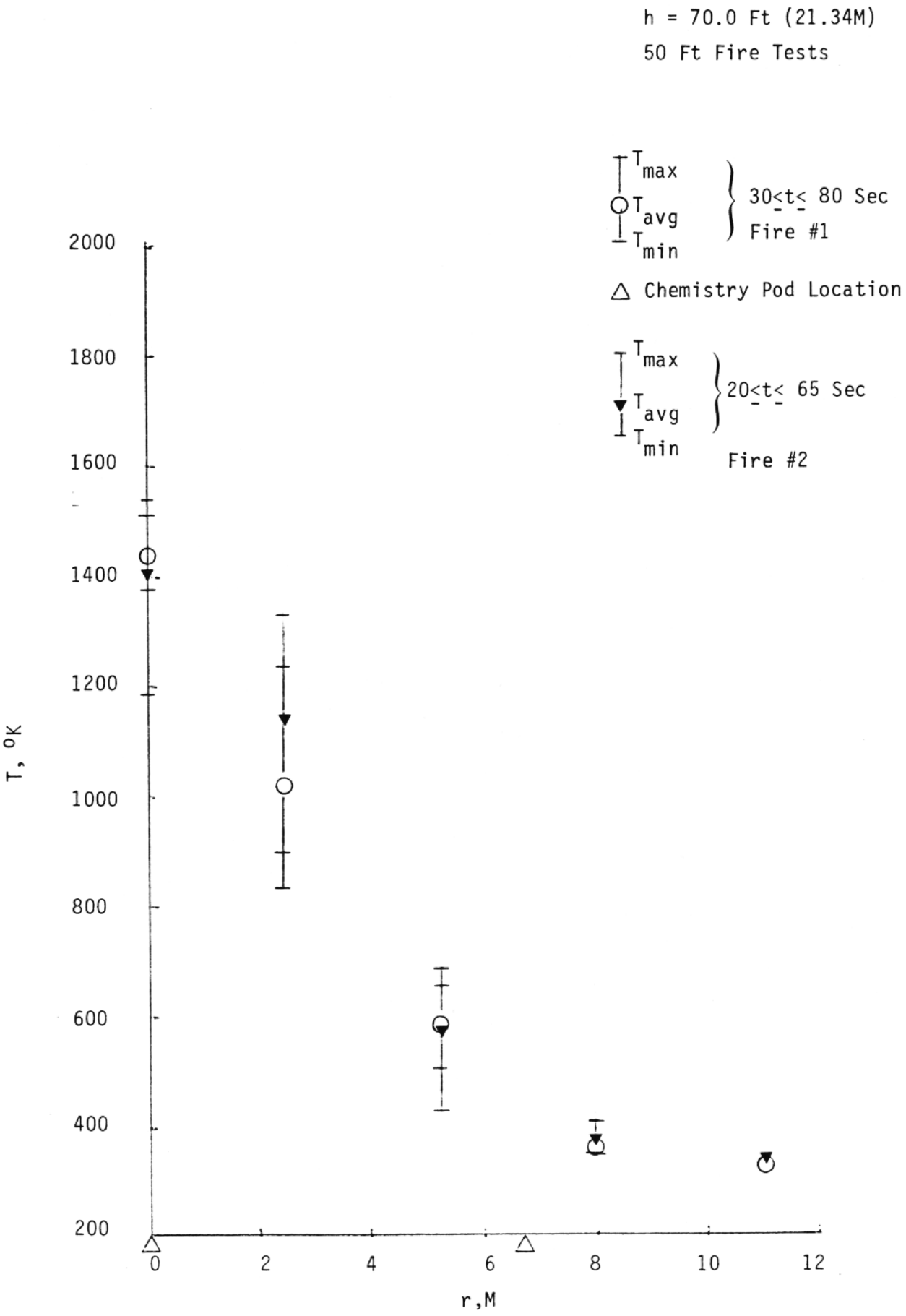

Figure 5. Experimental Radial Temperature Profiles, 15.24M (50 Foot) Fire Test, Height = 21.34M (70 Ft)

temperatures observed over the time interval of the measurements. The bands shown are thus not an indication of measurement inaccuracy (which was approximately $\pm 14^{o}K$) but of the large-scale unsteadiness of the flame.

Noteworthy from the data shown on Figures 1-5 is the excellent repeatability shown in the comparison between the two sets of data for the 15.24 meter (50 foot) fire, and the indication from the profiles that the fire was located approximately along the geometric centerline of the measurement apparatus in both cases. Also shown on these figures are the locations of the gas sampling apparatus for the first 50-foot fire test.

These data have been used to construct a composite representation of the observed flame flowfield. Using the measured radial profiles, axial temperature profiles can be constructed, such as the centerline (r=o) profile shown in Figure 6. By cross-plotting the results so obtained for a number of radial locations, an isothermal contour plot may be obtained, as shown in Figure 7, depicting the observed flame structure. From this representation, it can be seen that the tendency toward "necking down" of the flame isotherms noted in the initial fire computations (Ref. 1) is observed in the measurements. Also noticeable is a region of relatively high temperature located at a height of 3 meters and a radius of 2 meters. These local high temperatures may result from the complex entrainment and mixing processes occurring in this region and may be affected by the presence of the instrumentation structure in this region. Both of these possibilities will be investigated in further data analysis.

Gas sample data were also obtained at several locations within the fire, as noted on Figures 1-5. These measurements were made using an evacuated-chamber gas sampling technique, with samples drawn over a 20-30 second time span within the time span over which the temperature averaging was carried out. The samples were analyzed to obtain the mass fractions of the major constituent species in the fire, including oxygen, nitrogen,

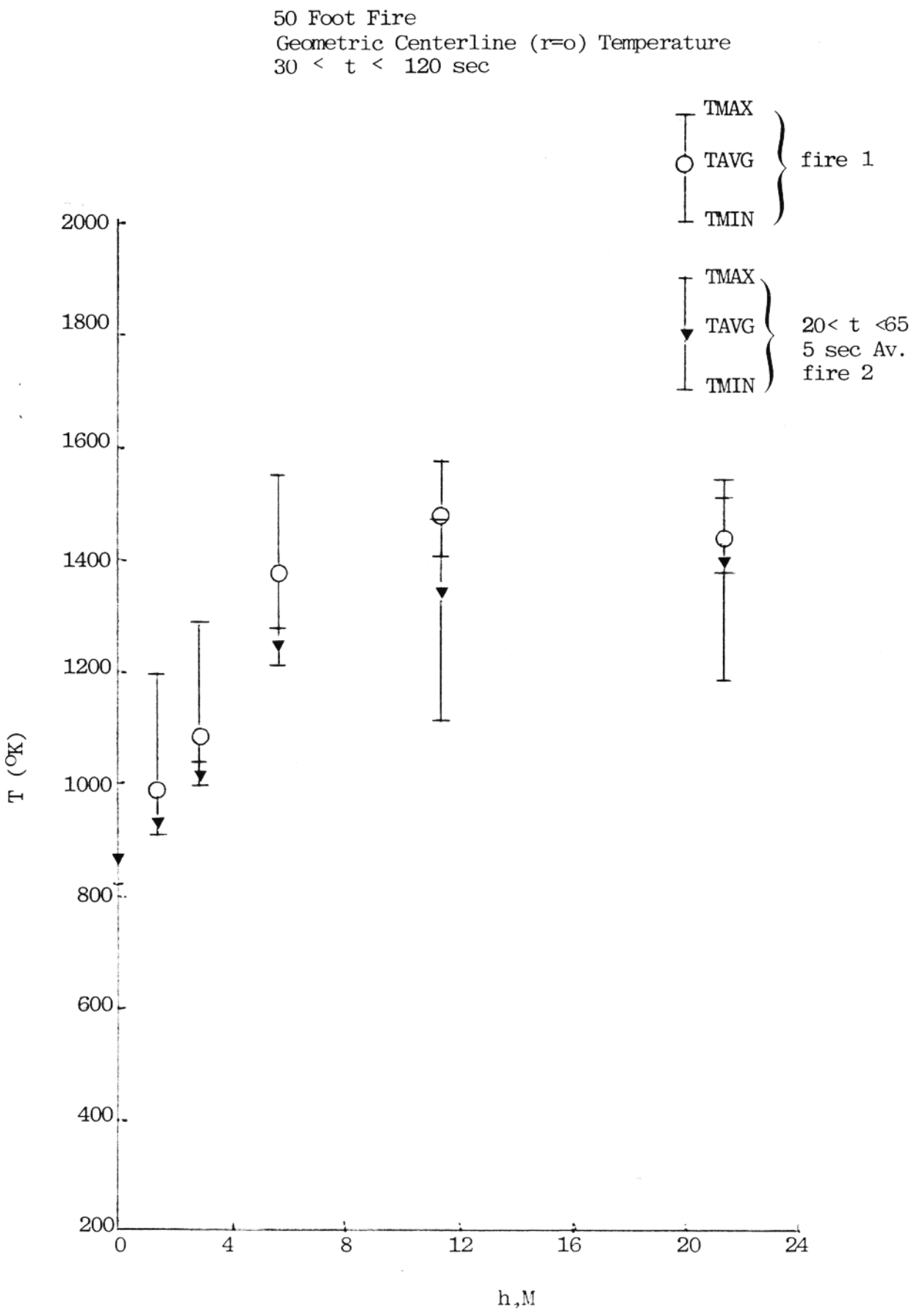

Figure 6. Experimental Centerline Temperature Profile, 15.24 M (50 Foot) Fire Tests

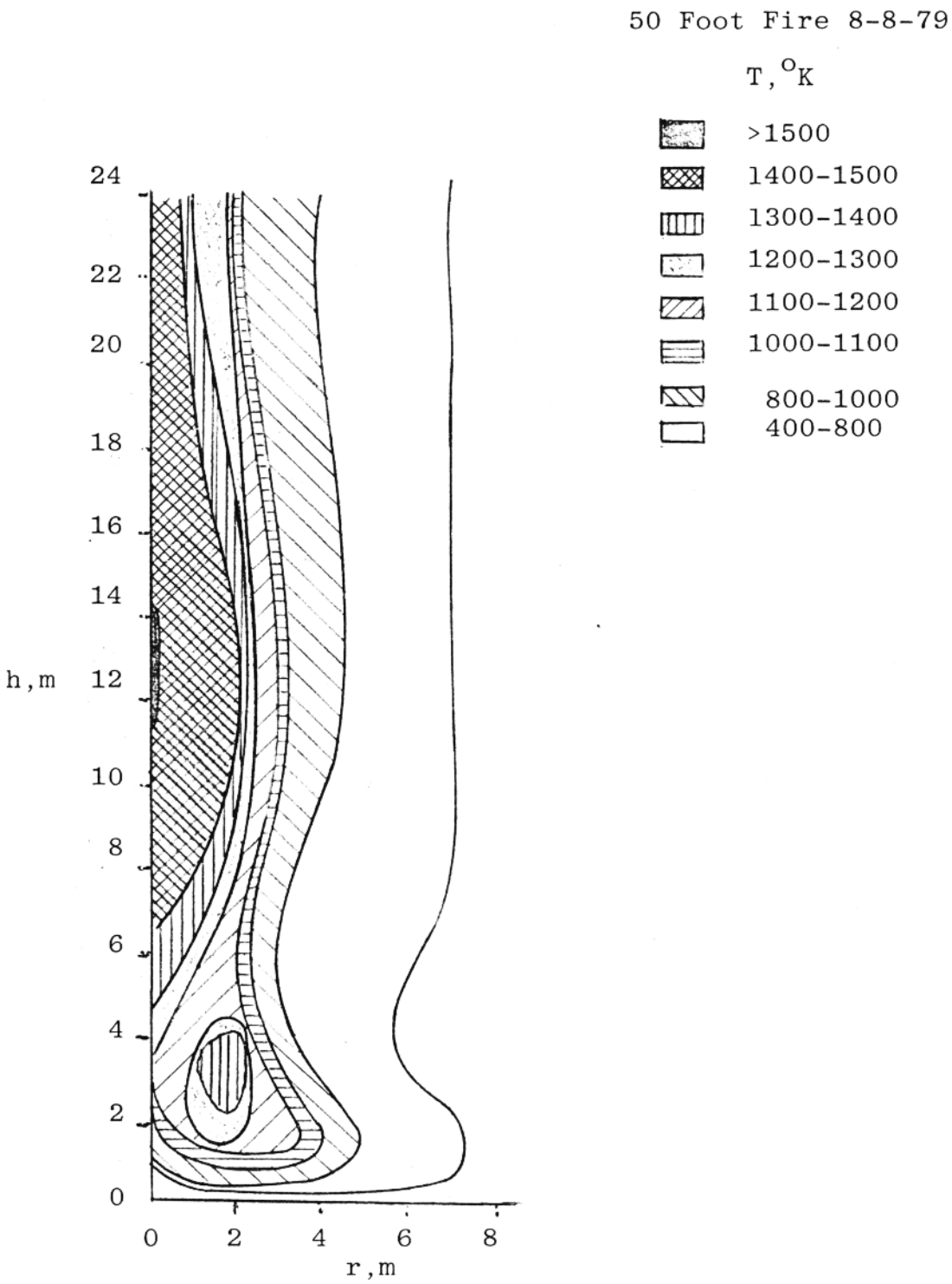

Figure 7. Isotherm Contours Obtained From Measurements In 15.24 M (50 Foot) Fire

hydrogen, water, carbon monoxide, carbon dioxide, argon, methane, higher gaseous hydrocarbons, condensed hydrocarbons, and soot. Analysis techniques and detailed data will be included in the forthcoming fire data report. Of particular interest from the standpoint of fire modeling and the computation of carbon fiber consumption within the fire are the local concentration of oxygen and fuel. Data for the mass fraction of oxygen and of fuel within the fire are shown in Fig. 8. In obtaining these results, the sample data were corrected for excess water vapor and the measured data for methane, higher gaseous hydrocarbons, and condensed hydrocarbons were lumped together as fuel mass fraction. Of interest in these data are the substantial fuel mass fractions observed within the fire even at the 11.43M (37.5 foot) height and the observed overlap of the fuel and O_2 mass fraction profiles. The former data can be interpreted (along with other results to be detailed in the forthcoming data report) as the result of a relatively slow breakdown of the fuel during the combustion process, while the latter results indicate a substantial unmixedness effect: the coexistence of fuel and oxidizer on a time average basis can be interpreted as the result of unmixed regions of fuel and oxidizer passing the sampling device at different times.

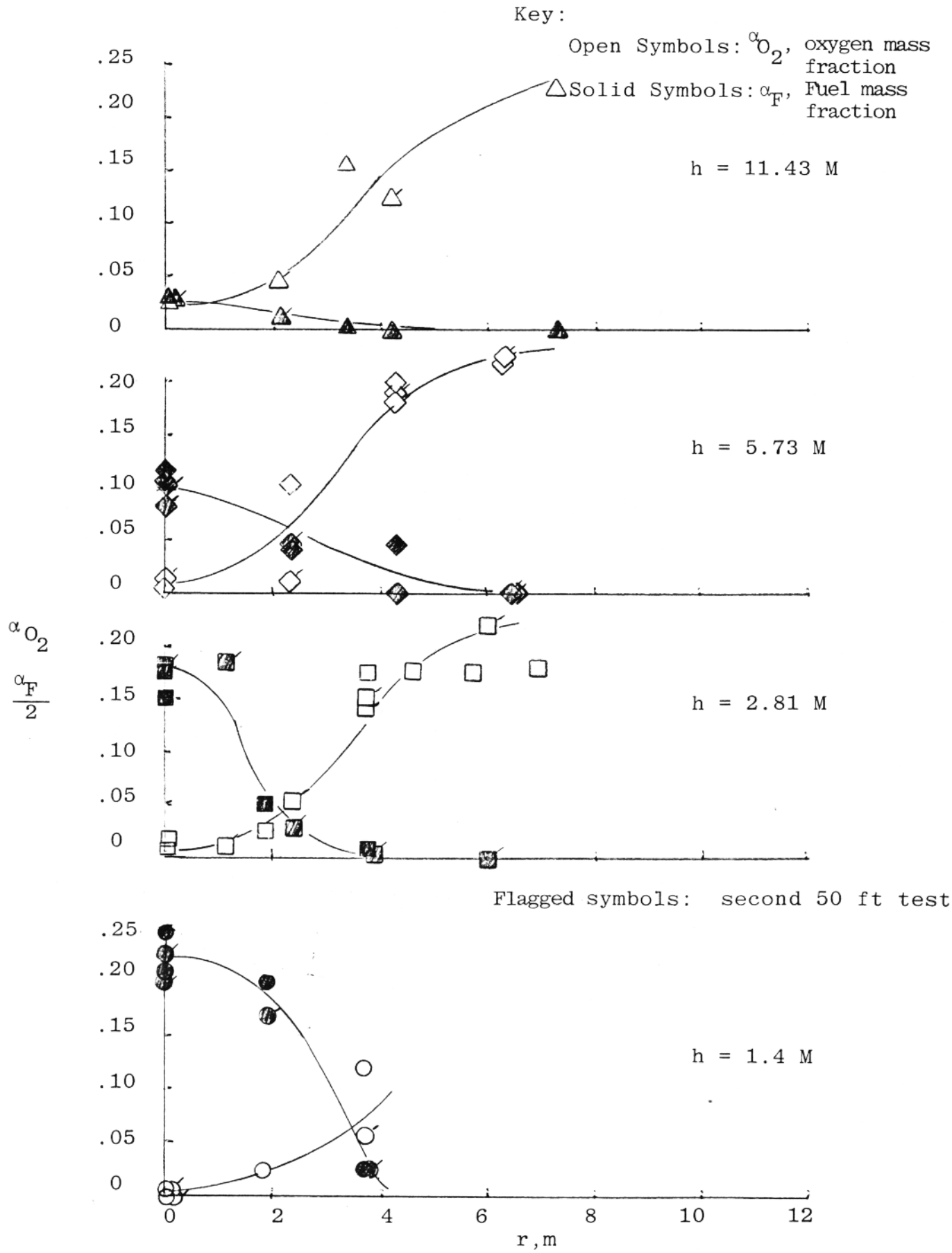

Figure 8 Measured Mass Fractions of Oxygen and Fuel, 15.24 M (50 Foot) Fire

Note: Curves drawn through data to illustrate trends

4. PRELIMINARY MODEL PREDICTIONS

Comparison of the data with the fire calculations reported in Ref. 1 showed that, while qualitative agreement was obtained, there were areas of quantitative disagreement. Specifically, the turbulent mixing rate of the fire was overpredicted, particularly in the higher regions of the fire, much higher peak temperatures were predicted than were observed, and the concentration measurements in the fire indicated substantial effects of unmixedness and incomplete combustion. Further, data on carbon fiber consumption obtained in separate experiments indicated that for the specific conditions of the experiments, carbon fiber consumption proceeded at a rate higher than that predicted by the Lee, Thring and Beer (Ref. 3) model.

Based on these comparisons, modifications to the initial fire fire model were made in three areas: the eddy viscosity model used to predict the turbulent mixing rate, the gas phase chemistry model, and the particulate consumption model. Each of these modifications is discussed below. In addition, the assumption of thermal equilibrium between the gas phase and particles inherent in the model described in Ref. 1 was relaxed to allow computation of fiber heat-up and continued combustion of fibers due to fiber temperature remaining greater than gas phase temperature in the upper fire region.

4.1 TURBULENT MIXING RATE

As noted in Section 2, a constant value of the eddy viscosity was used in the initial fire calculations. Comparison of the results obtained using this model with the data obtained during the 50 foot fire tests indicated that this model overpredicted the mixing rate, particularly at the higher fire elevations. This can be seen in Figure 9, which shows a comparison of the results of the initial fire model computation and two calculations carried out using a spatially varying eddy viscosity model with the 15.24 meter (50 foot) fire centerline temperature data. It is clear that the initial constant

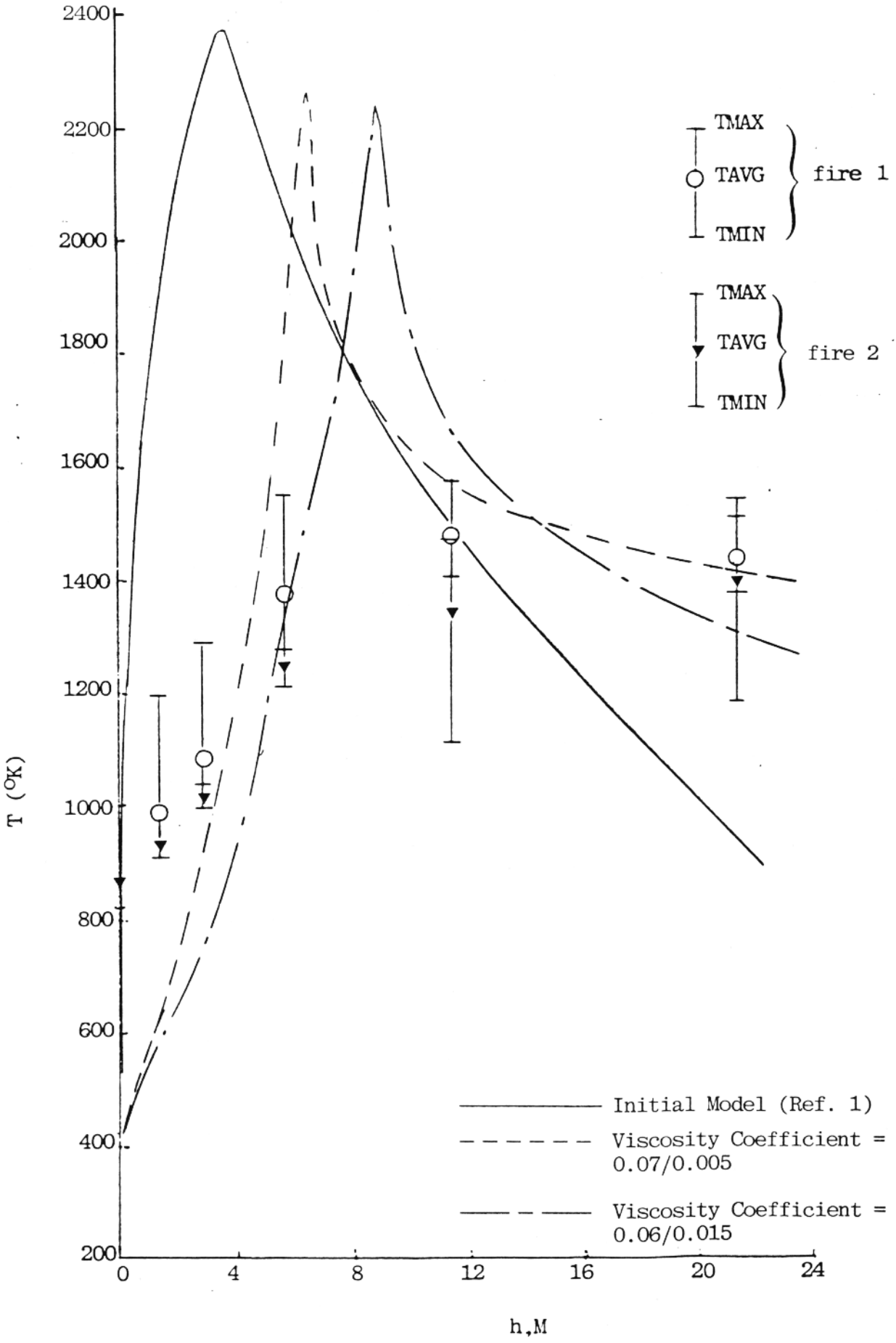

Figure 9. Effect of Variation of Eddy Viscosity Model And Eddy Viscosity Coefficients on Centerline Temperature Prediction, 15.24M (50 Foot) Fire

viscosity model is inadequate to represent the details of the fire as represented by these centerline temperature results. However, it can also be seen that the large mixing rate engendered by the high viscosity level used in the constant viscosity calculations is required to simulate the rapid temperature rise observed for heights less than 4 M. This requirement for large initial mixing rate cannot be met by a conventional jet-type eddy viscosity model. However, the model developed by Alpinieri (Ref. 4) was developed to simulate measurements made in a configuration in which very rapid initial mixing was observed, because of the presence of a small central recirculation region at the jet exit nozzle. Thus the Alpinieri model was applied to the prediction of this flowfield, with the model coefficients adjusted to provide the best fit with experimental data. As can be seen from Fig. 9, better results were obtained using a coefficient of 0.070 for $h < r_p$ (where r_p is the fuel pool radius) and 0.005 for $h \geq r_p$. It might be noted that the adjustment of coefficients to match experimental data is a common requirement when using locally dependent eddy viscosity models, and that the use of two coefficients for different flowfield regions is common in the use of eddy viscosity models to predict jet-like flows.

While in general the predictions using the model outlined above are in better agreement with the experimental data for centerline temperature than those of the model of Ref. 1, it can also be seen from Fig. 9, that all of the models predict a peak temperature level (2300°K) that is greater than observed in the data (see, for example, Fig. 7). This is a consequence of the chemistry model used in these calculations, and thus this area was the next investigated during the preliminary model modification effort.

4.2 GAS PHASE COMBUSTION MODEL

As noted in Section 3, the species mass fraction measurements of fuel and oxygen for the 15.24 meter (50 foot) fire show the spatial coexistence of both fuel and oxidizer within the flame. This can be interpreted as a result of the phenomenon of unmixedness within the flame, a phenomenon which was not accounted for in the modeling reported in Ref. 1.

Thus, a very simple unmixedness model was developed for use in this modeling work, primarily to assess the potential effects of unmixedness on the computed fire structure. This unmixedness model proceeds as follows:

It is assumed that because of unmixedness a part of the total oxygen element at every point in the flow is unavailable for reaction with the fuel, and that this fraction can be related to the local velocity fluctuation level, i.e.,

$$\tilde{\alpha}_{O_2 u} = fr \cdot \tilde{\alpha}_{O_2 t}$$

where

$$fr \propto \frac{u'}{U}$$

in which u' represents the root-mean-square (rms) axial turbulent fluctuation velocity and U is the mean axial velocity, so that fr is proportional to the local axial turbulent intensity. Then, since $\frac{u'}{U}$ can be related to the local turbulent kinetic energy level,

$$\frac{u'}{U} \propto \left(\frac{k}{U^2}\right)^{\frac{1}{2}}$$

and noting that, consistent with the use of a locally dependent eddy viscosity model turbulent energy production can be related to turbulence energy dissipation

$$\frac{\rho\, a_2 k^{3/2}}{l_k} = \mu_t \left(\frac{\partial u}{\partial r}\right)^2$$

a relationship for fr can be obtained:

$$fr = f \cdot \left(\frac{\mu_t l_k}{\rho}\right)^{1/3} \left(\frac{\partial u}{\partial r}\right)^{2/3}$$

where μ_t is the local turbulent viscosity, l_k a length scale taken to be

that used to obtain the local turbulent viscosity, ρ is the local density and f a coefficient which is to be evaluated through comparison of predictions with data. Thus, at each point in the flow a fraction of the total oxygen element which is unavailable for use in the complete-combustion gas phase chemistry calculation can be computed. While this model is dependent on a number of simplyifying assumptions, and is applied in this work to the oxygen only (and not to the fuel) it can be used to assess the effects of unmixedness on the fire structure computation. Further development of this unmixedness approach will be undertaken in subsequent work.

Comparisons of the predictions using the fluctuating chemistry model with measured temperature data are shown in Figs. 10-15. Figure 10 provides a comparison of the predicted centerline temperature profiles with the experimental data for three values of the parameter f. The decreased temp-atures observed on the axis for f=0.5 compared to f=1.0 and f=1.5 may be related to increased overall mixing rates obtained using f=0.5 for heights less than 5.78 meters. While peak temperature levels (Figures 11 and 12) have been reduced from $\sim$2400^{o}K to 1800-2000^{o}K through the use of simple unmixedness model they are still substantially higher than the observed temperatures at the 1.43 meter and 2.87 meter heights. However, it should be noted that compared to calculations made with no unmixedness effects, these computations have a considerably reduced spatial region in which higher than observed peak temperatures are obtained. This is of importance with relation to the fiber consumption results described in Section 5 of this report, since the residence time of the fibers in unrealistically high temperature flame regions is substantially lower in these computations than in computations neglecting unmixedness. The computed peak temperatures, and the measured presence of fuel at heights as great as 11.43 meters, indicate that in subsequent work the fluctuating chemistry model should be applied to the fuel as well as the oxidizer. Overall, the results shown on Figures 10-15 indicate that f=0.5 provides the best overall agreement with the temperature data from the two fire tests. Comparison of the computed results with the data for $h \leq$ 5.73 meters is further affected by the presence of the instrumentation structure within the fire. The fluid-dynamic effects of this structure have not been directly accounted for in the analytical model.

50' fire Center Line

Curves are from calculations using the fluctuating chemistry model.

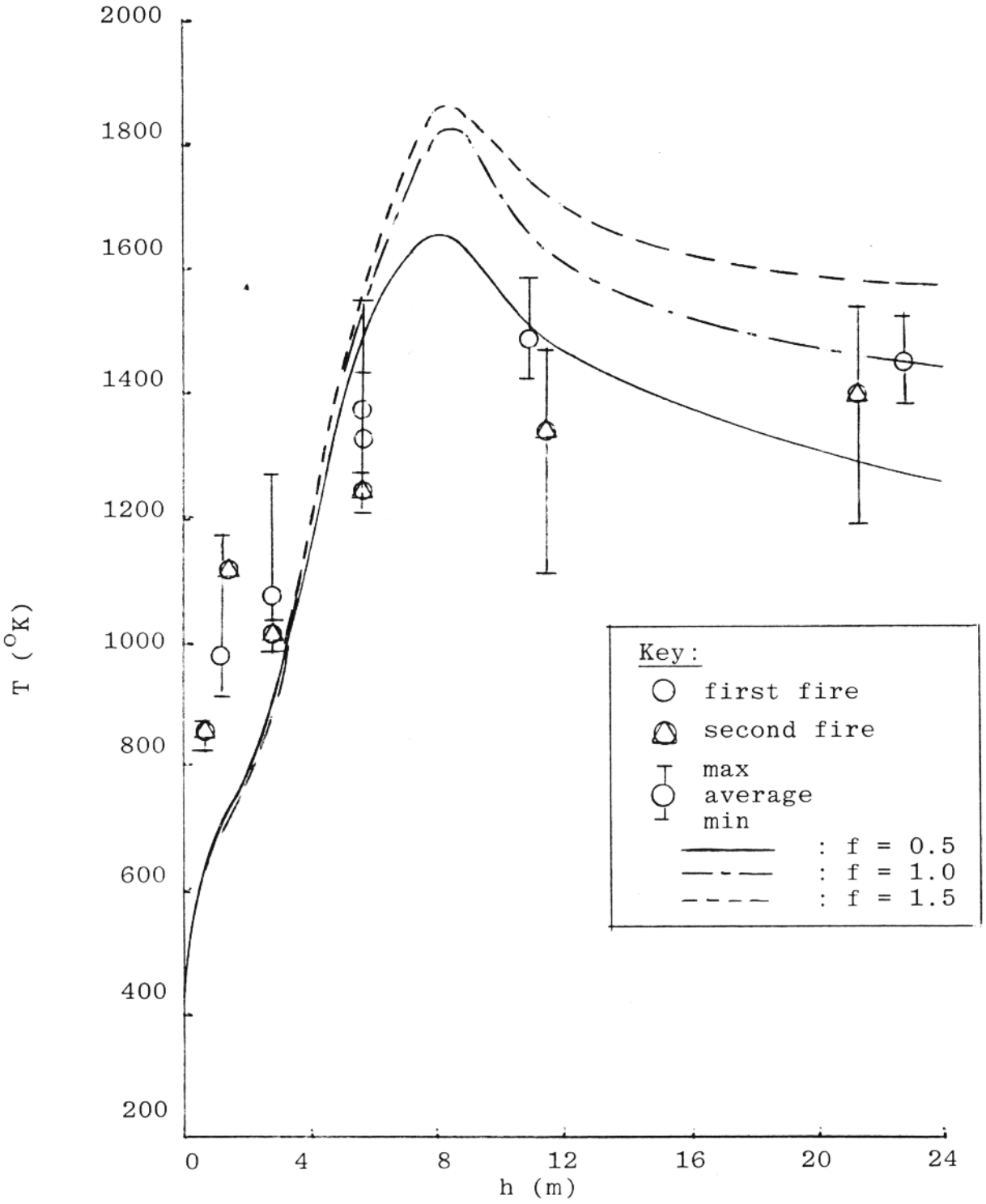

Figure 10: Comparison of Computations Incorporating Fluctuating Chemistry Model With Centerline Temperature Data.

50' fire Height=1.433 meters

Curves are from calculations using the fluctuating chemistry model

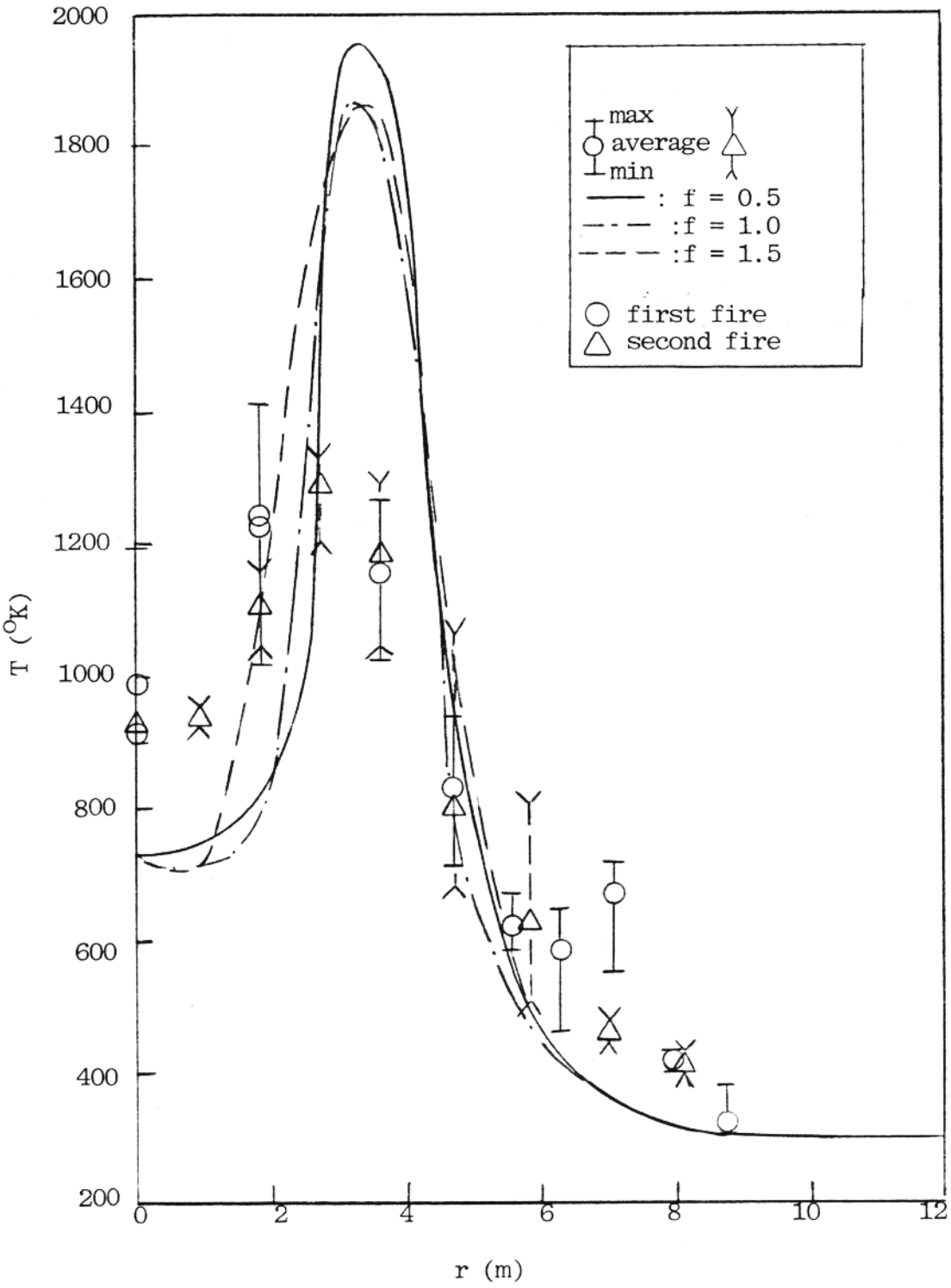

Figure 11. Comparison of Computations Incorporating Fluctuating Chemistry Model With Radial Temperature Data, h=1.433 meters.

50' fire Height=2.87 m

Curves are from calculations using the fluctuating chemistry model

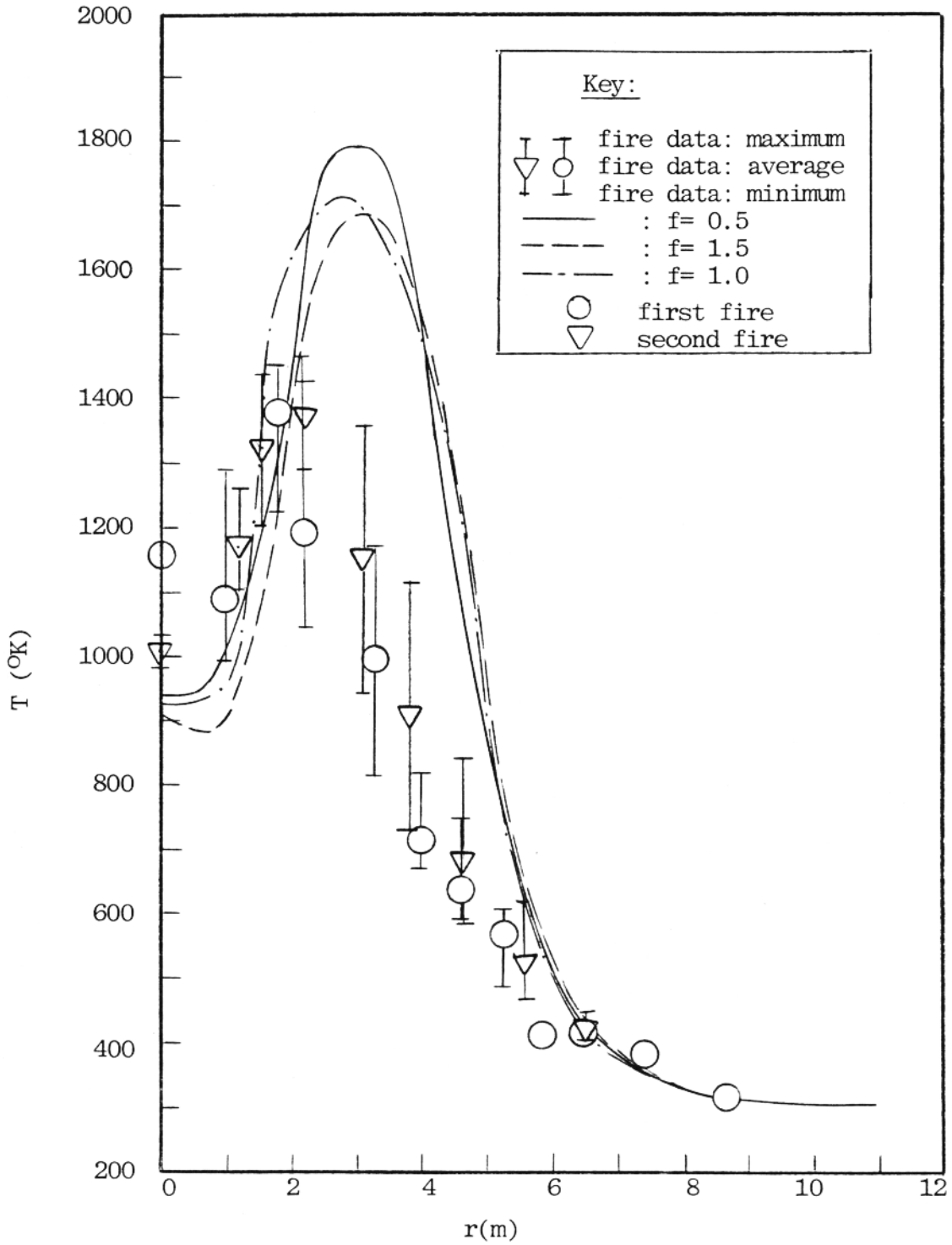

Figure 12. Comparison of Computations Incorporating Fluctuating Chemistry Model With Radial Temperature Data, h=2.87 meters

50' fire Height=5.73 M

Curves are from calculations using the fluctuating chemistry model

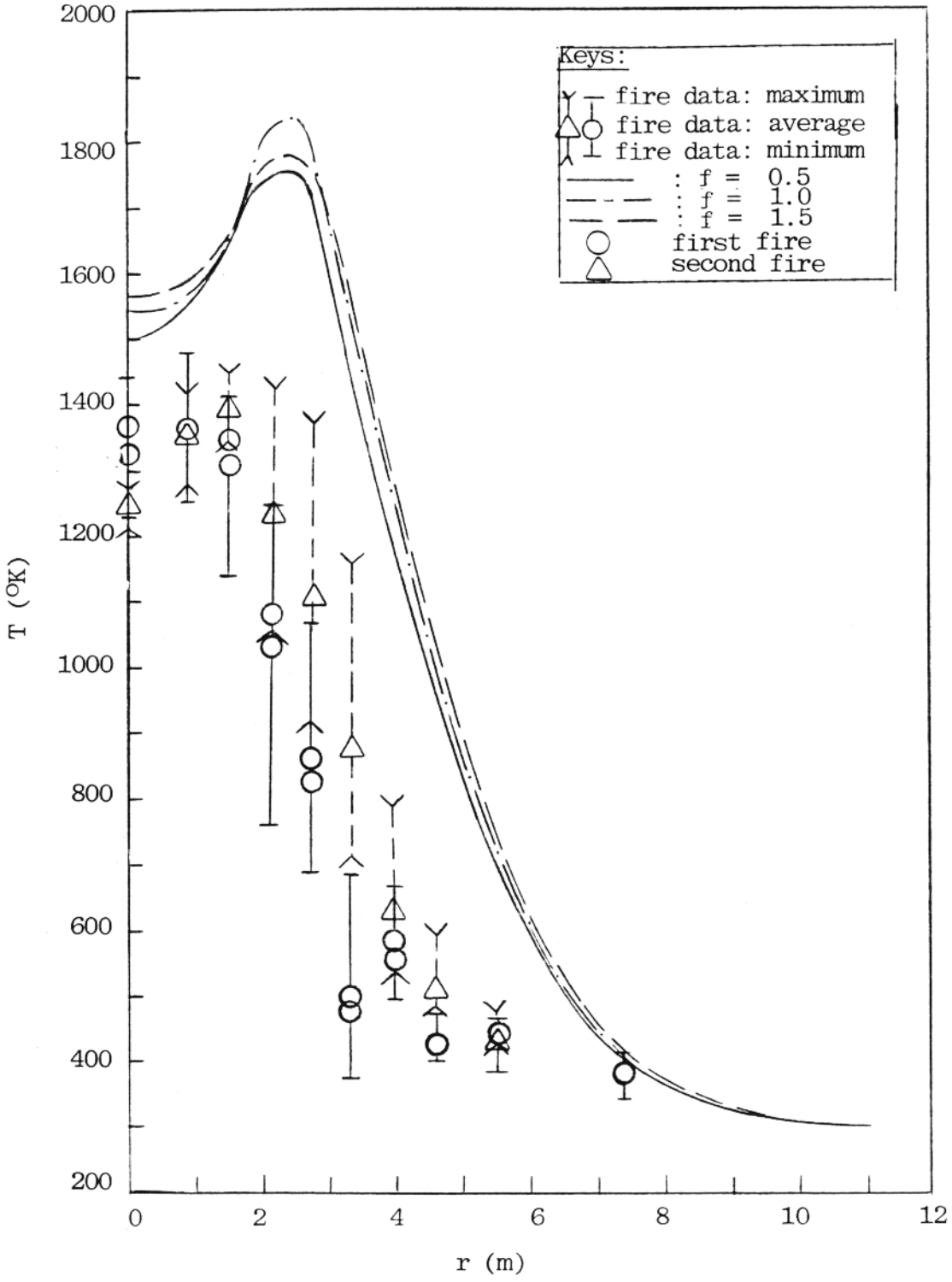

Figure 13. Comparison of Computations Incorporating Fluctuating Chemistry Model With Radial Temperature Data, h =5.73 meters.

50' fire Height=11.43 M

Curves are from calculations using the fluctuating chemistry model

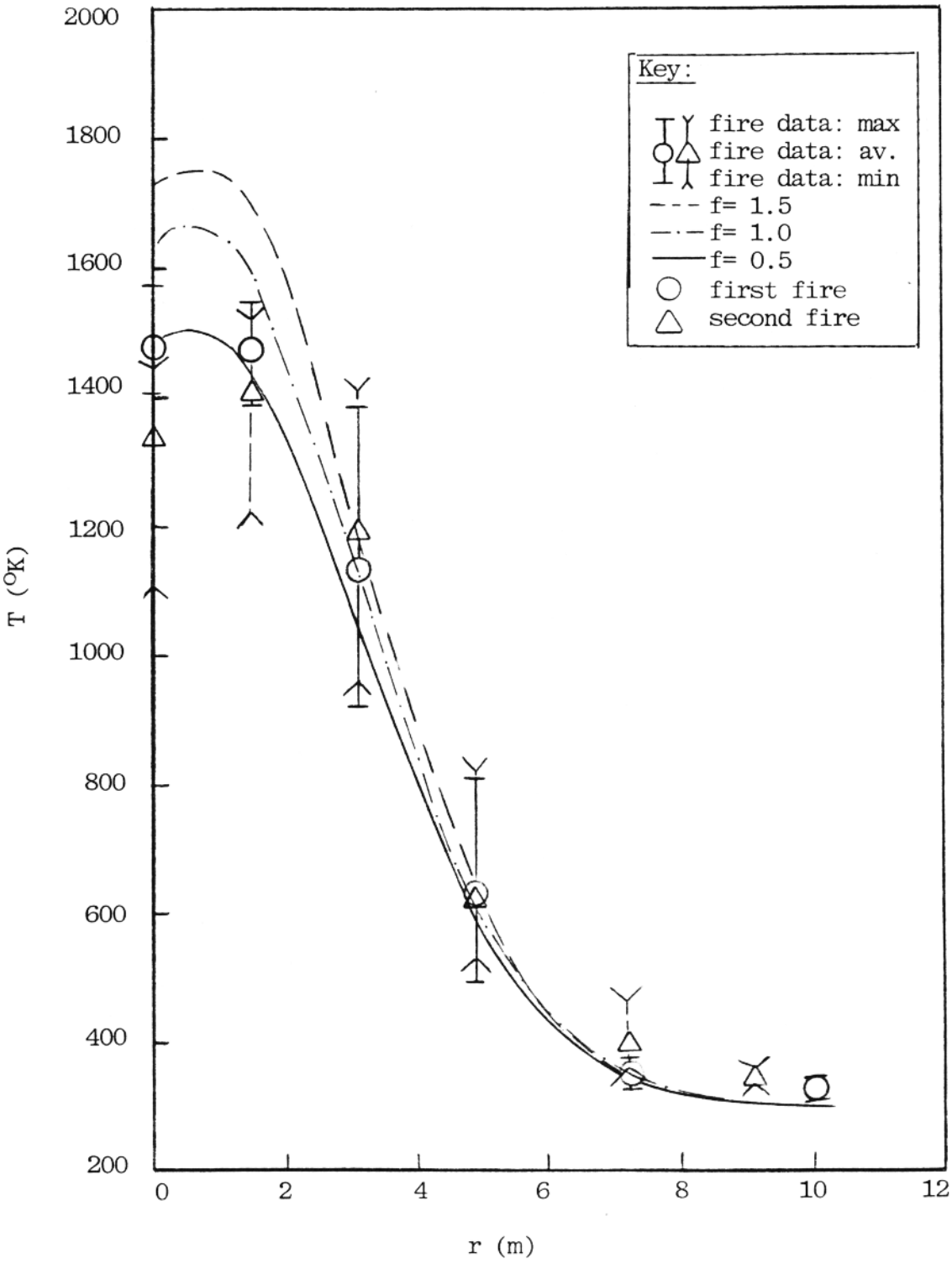

Figure 14. Comparison of Computations Incorporating Fluctuating Chemistry Model With Radial Temperature Data, h=11.43 meters.

50' fire Height=21.3m

Curves are from calculations using the fluctuating chemistry model

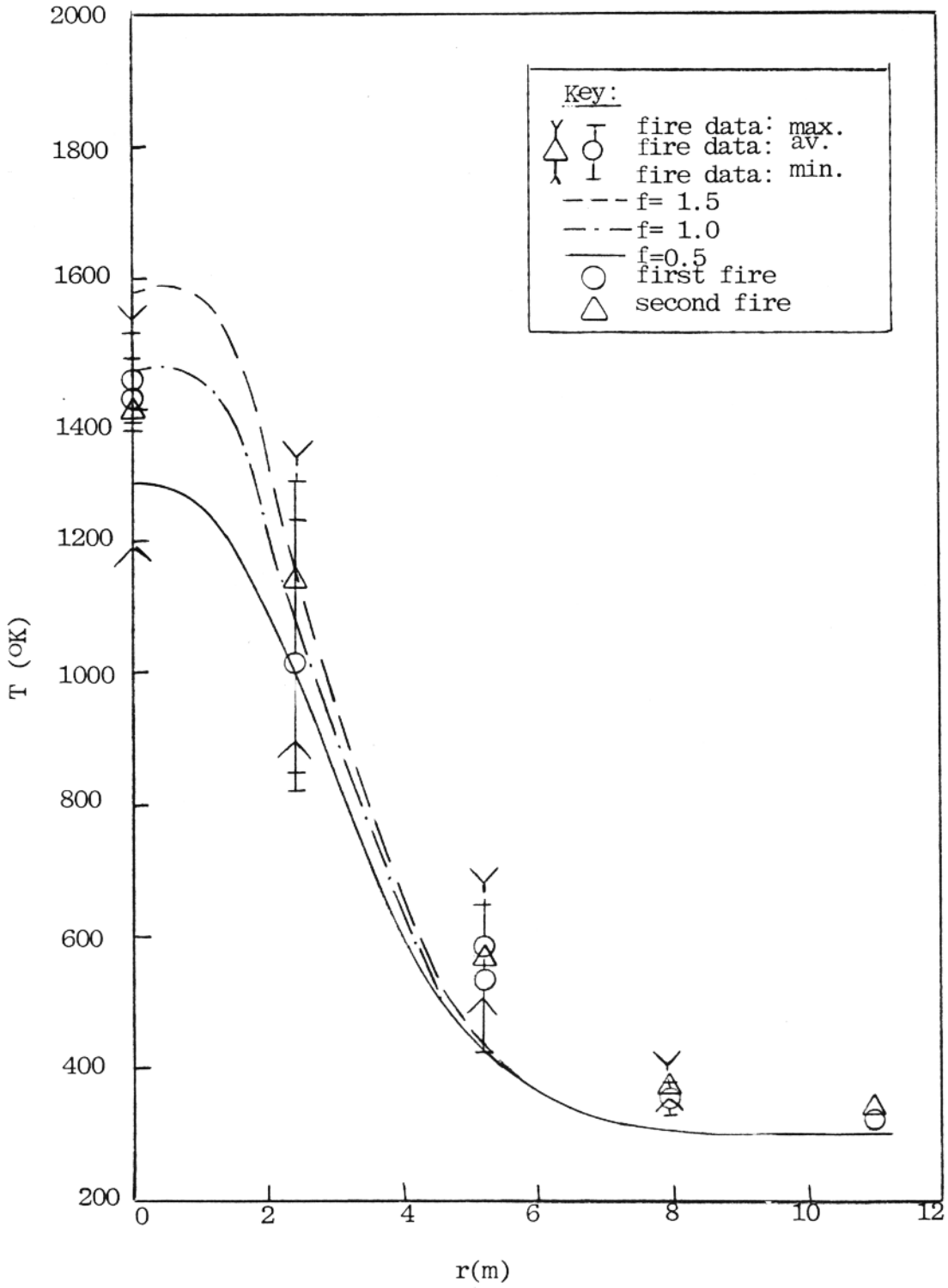

Figure 15. Comparison of Computations Incorporating Fluctuating Chemistry Model with Radial Temperature Data, h=21.3 meters.

In addition to its effect on the predicted temperature profiles, the incorporation of a fluctuating chemistry model also allows the presence of O_2 in fire regions where the basic (complete combustion) chemistry model does not allow oxygen to exist. This is illustrated in Figure 16, from which it can be seen that at heights less than 11.43 meters, the basic combustion model does not allow the presence of O_2 near the centerline. The fluctuating model results do, on the other hand, show small amounts of O_2 near the centerline, and these amounts, though small, could have an impact on the amount of fiber oxidation in the fire.

4.3 FIBER CONSUMPTION MODEL

The Lee, Thring and Beer (Ref. 3) model for the consumption of soot particles was utilized in the fire modeling described in Ref. 1 to predict fiber consumption rates. In this work, the fiber consumption model has been modified to reflect the results of work done at NASA Langley on individual fiber consumption rates as a function of temperature and oxygen partial pressure. However, only one set of data, for a temperature range of 450°C to 700°C and an oxygen partial pressure of 0.0816 atm was suitable for the development of a fiber oxidation rate expression. Thus, while a modified rate expression was developed from these data as shown on Figure 17, it can only be considered to be preliminary as the possibly substantial effect of oxygen partial pressure on the rate has not been determined. Further, the experiments involve a variable particle heat up time during which some consumption is occuring. This variable heat up time cannot be incorporated into the development of the model for particle consumption. Finally, possible physical differences (e.g., surface coatings) between the test particles and those released in a fire

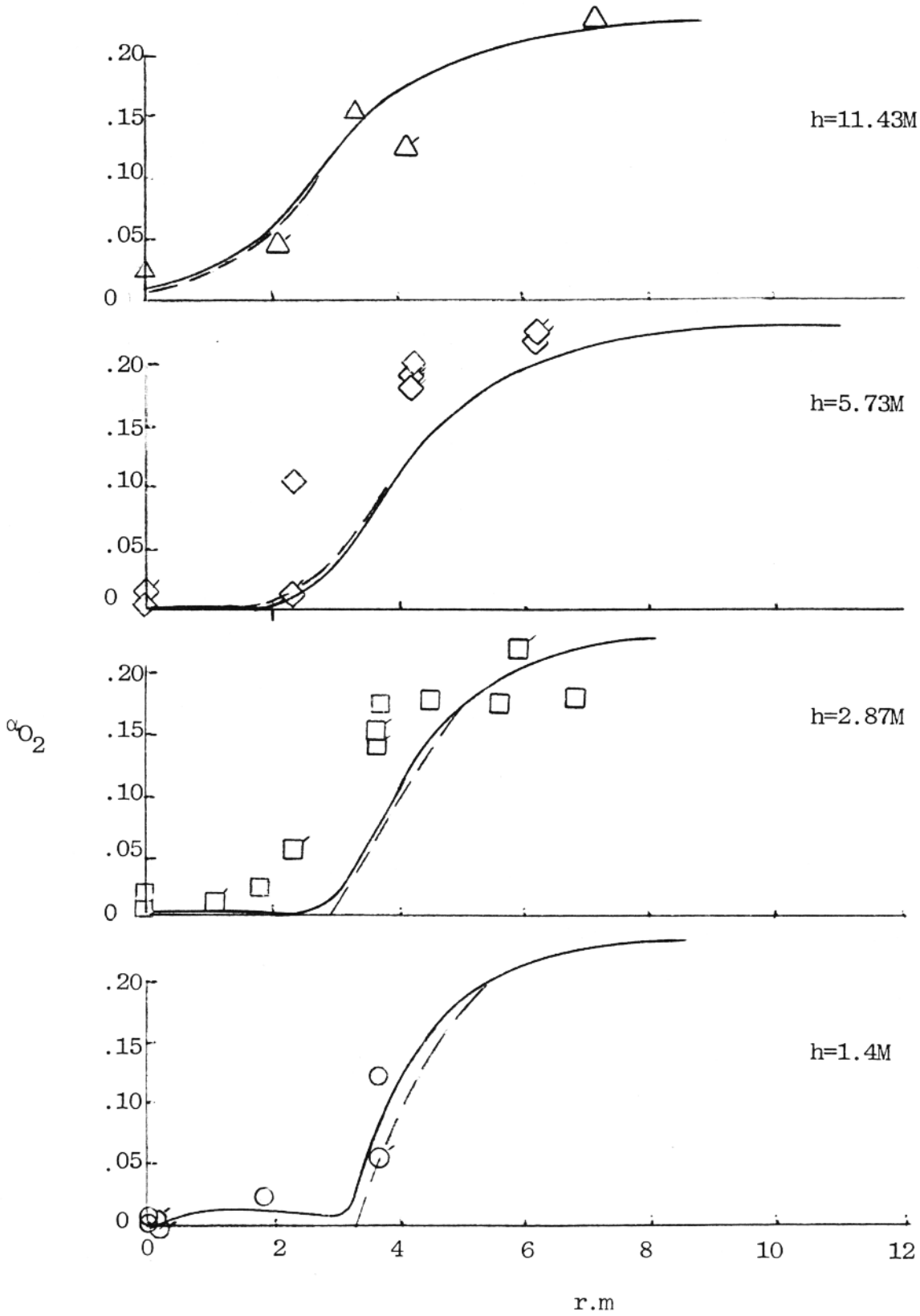

Figure 16. Comparison of Predicted And Measured O_2 Concentrations, 15.24 meter (50 foot) fire

——— With fluctuating Chemistry

— — — Without Fluctuating Chemistry

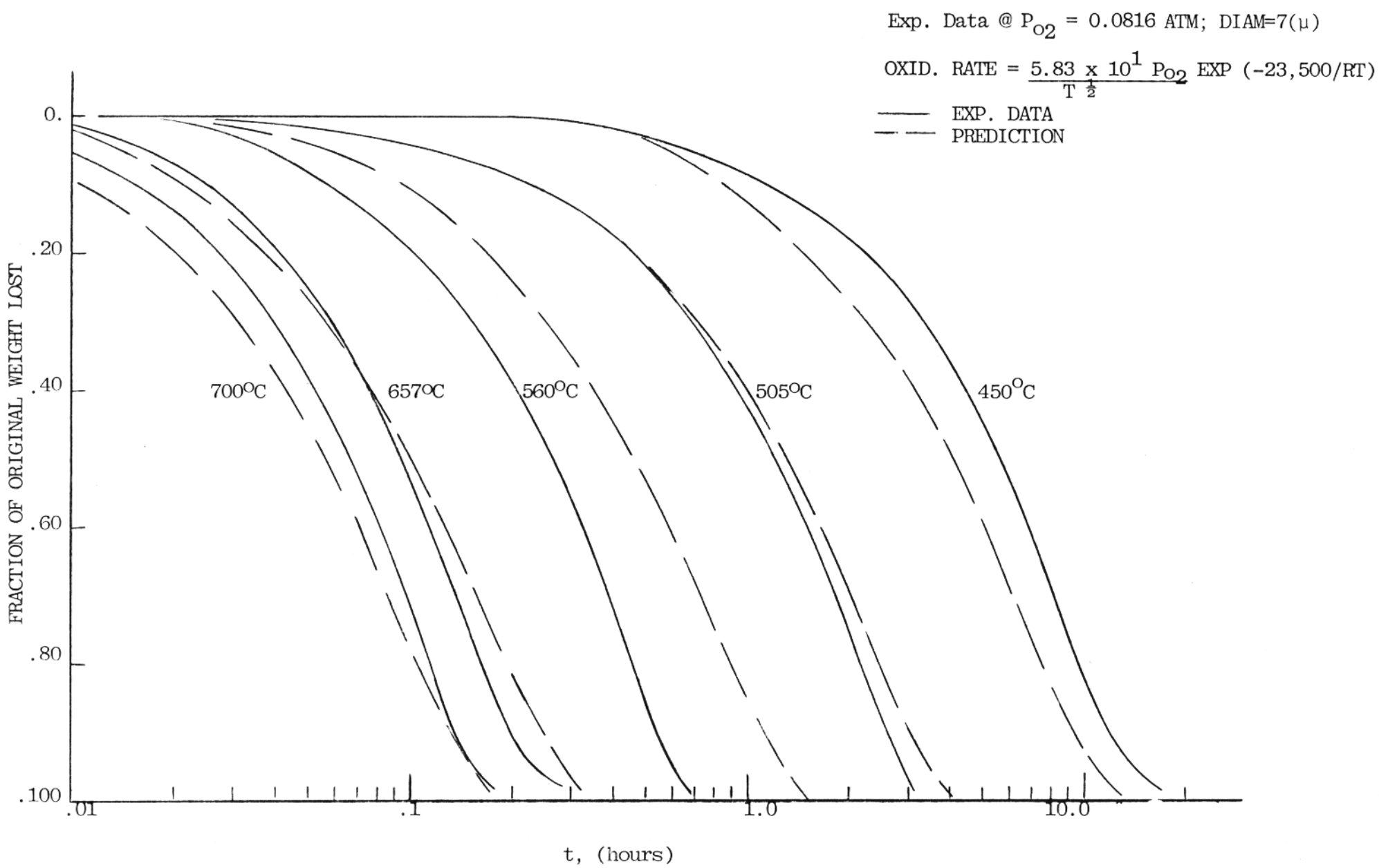

Figure 17. Comparison of Modified Lee, Thring, and Beer Model with Fiber Consumption Data.

have not been investigated. All of these uncertainties can lead to substantial differences between predicted and measured particle consumption rates in a fire environment and should be investigated in subsequent work.

4.4 FIBER THERMAL NONEQUILIBRIUM

The computations reported in Ref. 1 were all carried out under the assumption of fiber thermal equilibrium, that is, that the fibers are everywhere the same temperature as the gas phase. For some of these calculations this assumption has been relaxed, so that the heating and subsequent cooling of the fibers in response to the gas phase temperature change can be computed. This is done by writing a particle-phase energy transport equation for each particle class, which includes as source terms expressions representing the heating of the particle by conduction from the gas phase, energy loss from the particle caused by radiation, and heating of the particle caused by surface combustion, all of the energy of which is assumed to be absorbed by the particle.

During the course of the development of the thermal nonequilibrium model, a number of one-dimensional single fiber computations were carried out which are of interest with regard to the response of the fibers to temperature changes and the effects of surface combustion on particle temperature. Figure 18 depicts the response of a single fiber to gas-phase temperature change considering only conduction heat transfer (which is, however, the largest single contribution by a substantial amount). For this calculation, the initial gas-phase temperature (T_{g_o}) was 1500°K, and the initial fiber temperature (T_{p_o}) was 300°K. Under conduction only conditions, and assuming that the particle specific heat and gas conductivity are constants, an analytical solution can be obtained; in the numerical solution both conductivity, λ, and heat capacity, C_{p_p}, are functions of the gas phase and particle temperatures, respectively. Figure 18 shows that the 1/e response time of the fiber is about 0.10 seconds. Within the fire, there may be regions of locally high (i.e., near stoichiometric) temperatures on scales of the order of 0.01 d_F, where d_F is the local fire diameter. If such high temperature regions exist, and

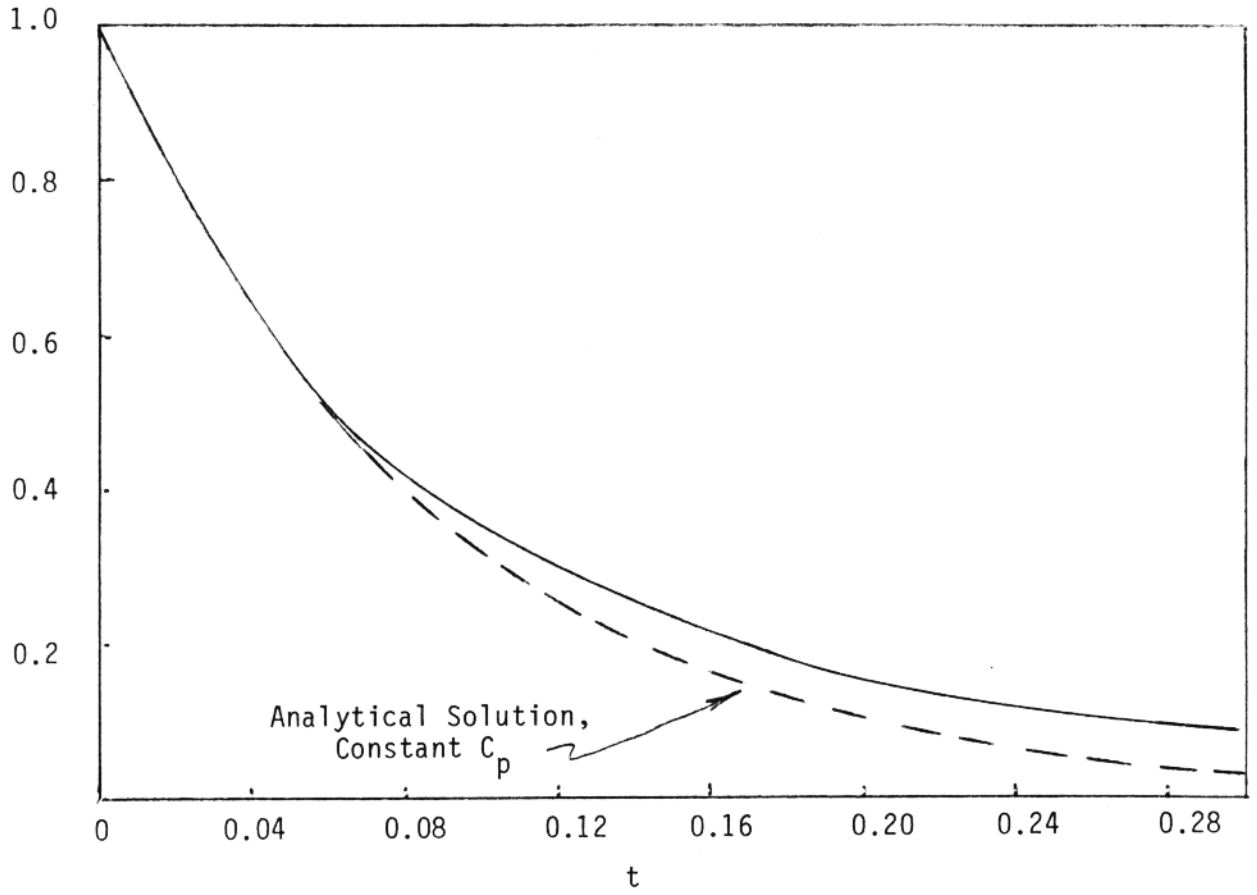

Figure 18. Response Of A Single Fiber To Gas-Phase Temperature $T_{p_o} - T_{g_o}$ = 1200°K, Conduction Only

a local fire diameter of the order of one-half the pool diameter is assumed (Fig. 7), and it is further assumed that these eddies have a convection velocity relative to the mean velocity of the order of $0.1\bar{U}$, then a "hot" eddy lifetime is of the order of 0.03 seconds. Comparison of this lifetime with the single-fiber response time of 0.10 seconds indicates that the fibers are essentially unaffected by local temperature fluctuations.

Additional one-dimensional calculation results including the effects of thermal radiation and particle consumption are shown on Fig. 19. As can be seen from this figure, the inclusion of radiation has a negligible effect on the temperature history; and the incorporation of particle combustion also leads, for these conditions, to negligible changes relative to the conduction only solution.

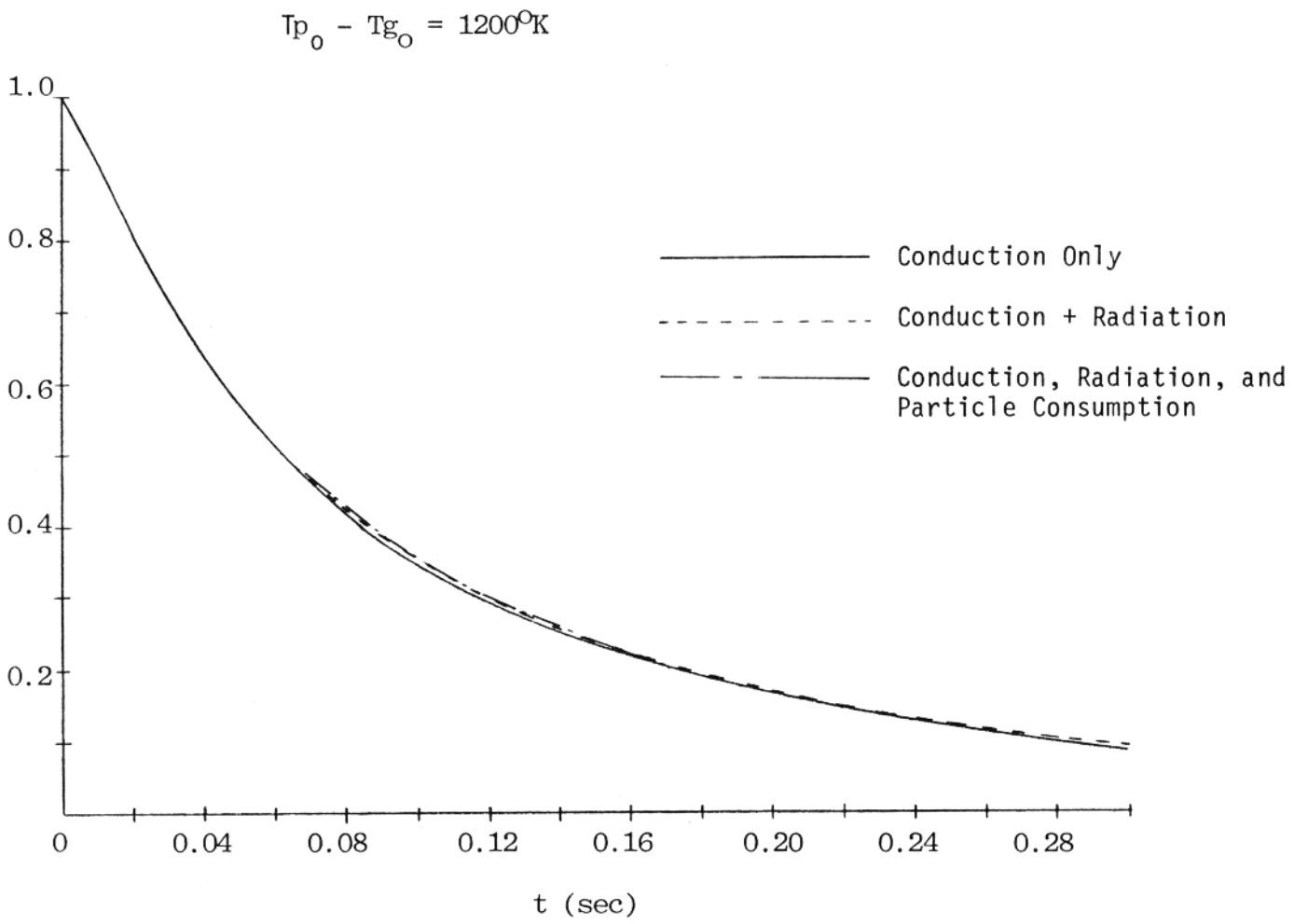

Figure 19. Effects of Radiation and Particle Combustion on Fiber Temperature History

5. PREDICTION OF FIBER FLUXES AND CONSUMPTION

Based on the results of this preliminary model modification effort, a mathematical model for large open fires has been developed which, relative to the model described in Ref. 1, includes:

1. Improved eddy viscosity model for the turbulent mixing process.
2. Modeling to include the effects of unmixedness on the gas phase chemistry.
3. Modified consumption rate expression for single fibers based on empirical data.
4. Thermal nonequilibrium between particles and gas phase.

This modified model has been applied to the computation of carbon fiber fluxes for three pool fire sizes: 7.62 meters (25 feet), 10.67 meters (35 feet) and 15.24 meters (50 feet); carbon fiber consumption was computed for the 7.62 meter and 10.67 meter fires. Similar initial conditions were used for all fire calculations: fuel vaporization rate of 8.5×10^{-3} cm/sec (0.20 in/min particle release rate of 10kg/min, distributed uniformly across the pool*, a fuel vapor temperature of 400°K and an ambient temperature of 300°K. The particle characteristics for these computations were as follows:

Particle Class	r_p(cm)	ℓ_p(cm)	f_p(kg/min)	Remarks
1	3.5×10^{-4}	0.15	0.288	Single Fiber
2	3.5×10^{-4}	0.35	0.448	Single Fiber
3	3.5×10^{-4}	0.65	0.791	Single Fiber
4	3.5×10^{-4}	1.00	1.217	Single Fiber
5	3.5×10^{-4}	1.40	1.076	Single Fiber
6	3.5×10^{-4}	5.00	3.202	Single Fiber
7	3.5×10^{-4}	25.0	1.282	Open Fiber Cluster Long Single Fiber
8	5.12×10^{-3}	10.0	1.694	Large Fiber Cluster

*The work reported in Ref. 1 showed that initial location of the fibers has no significant effect on the fiber fluxes within the fire.

5.1 FIBER CONSUMPTION PREDICTIONS

An issue of some concern is the possibility of significant consumption of the carbon fibers within the fire itself. In order to evaluate this possibility, computations were carried out for two fire sizes with the fiber consumption model described in Section 4.3 incorporated in the model. In view of the thermal nonequilibrium results reported in Section 4.4, the thermal equilibrium assumption was retained in these calculations. Results, expressed as percent of total fibers consumed, are shown for the single fibers in Figure 20: single fiber results are shown because these fibers are much more readily characterized in terms of geometric parameters (length, diameter, effective surface area, volume) than are the fiber clusters and clumps. These results show that the bulk of the fiber consumption occurs in the lower regions of the fire. For the larger fire, the initial consumption at a given value of height above the liquid fuel pool is lower than for the smaller fire since the height at which the peak temperature occurs increases with pool diameter. It is also evident that the total fiber consumption increases somewhat with fire size, and that in both cases fiber consumption has ceased by the 60 meter (200 ft) height in the fire.

5.2 FIBER FLUX PREDICTIONS

Fiber flux results for the single fibers are presented for three fire sizes in Figures 21-23. These results are presented as local fiber fluxes (kg/m^2-sec) normalized with initial fiber flux: since the burning rate for all single fibers is the same, because of the assumption that the surface area of the ends of a cylindrical fiber can be neglected in the consumption calculation, and it has been assumed in these computations that all single fibers have the same turbulent diffusivity, these normalized curves can be used to relate the flux of any class of single fibers to its initial flux. The initial fiber flow rates used to generate these computational results have been tabulated at the beginning of Section 5.

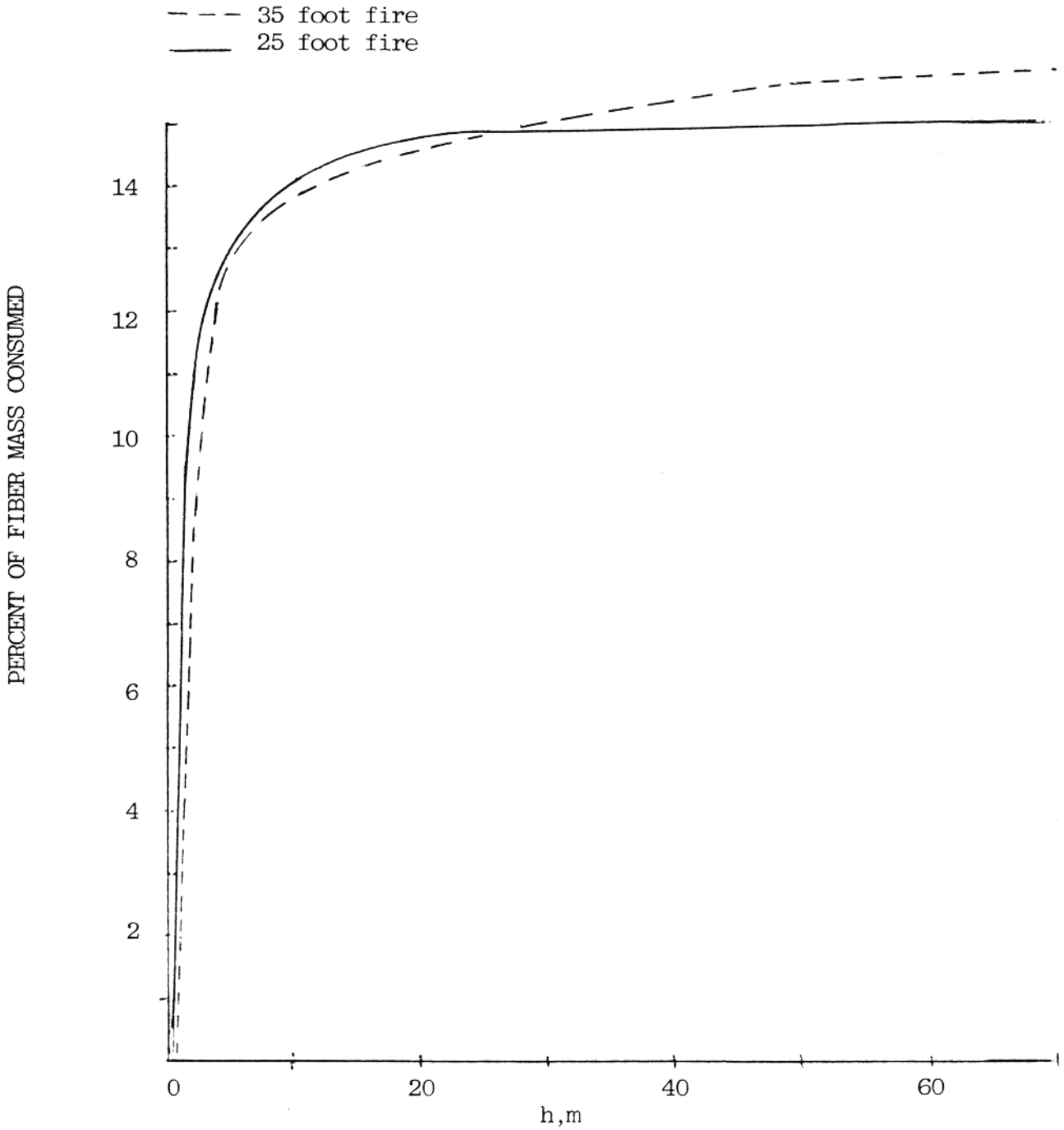

Figure 20. Fiber Consumption (single fibers) Computed for Two Fire Sizes

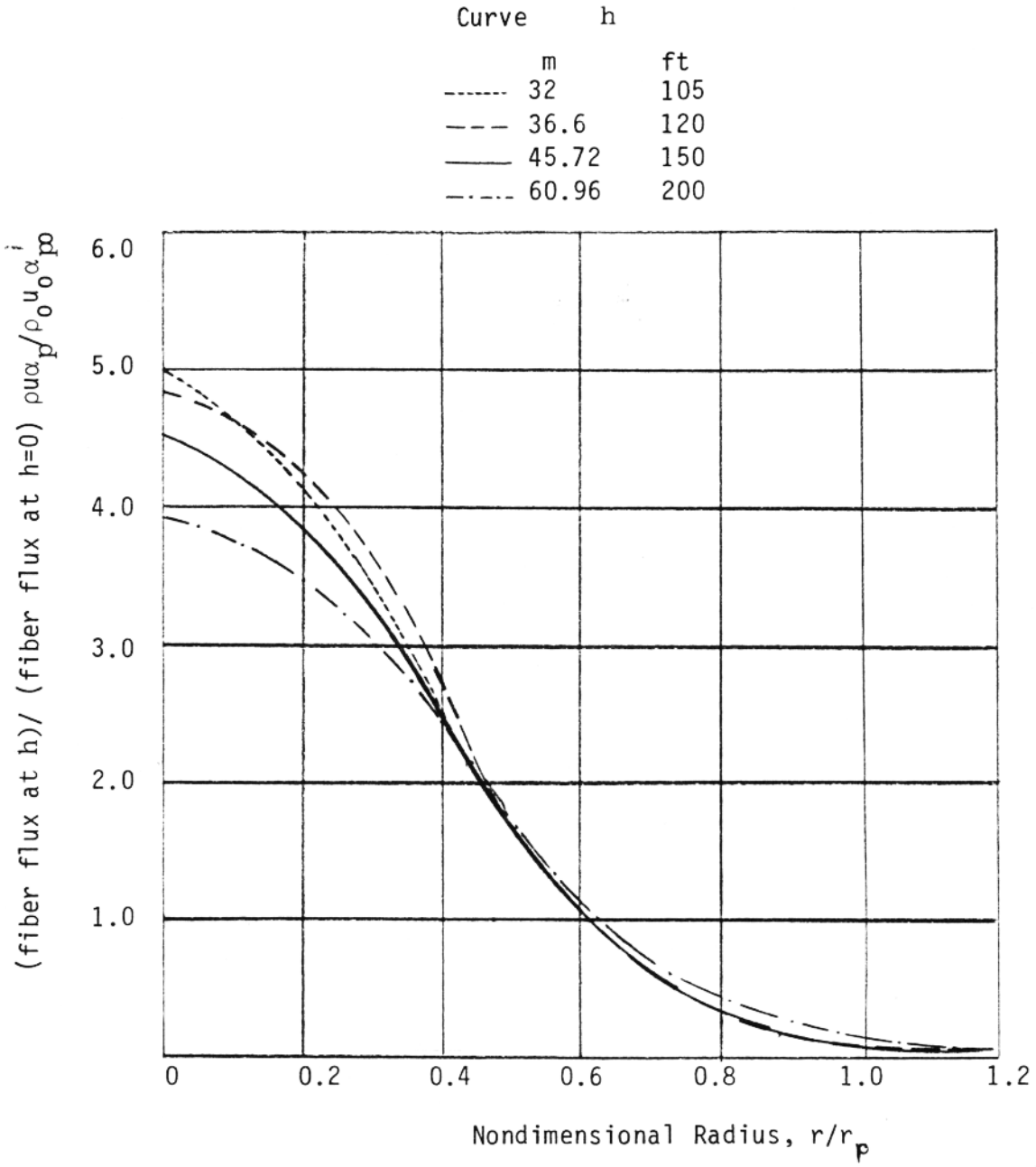

Figure 21. Normalized Fiber Flux Profiles as a Function of Height, 7.5M (25 foot) diameter fire

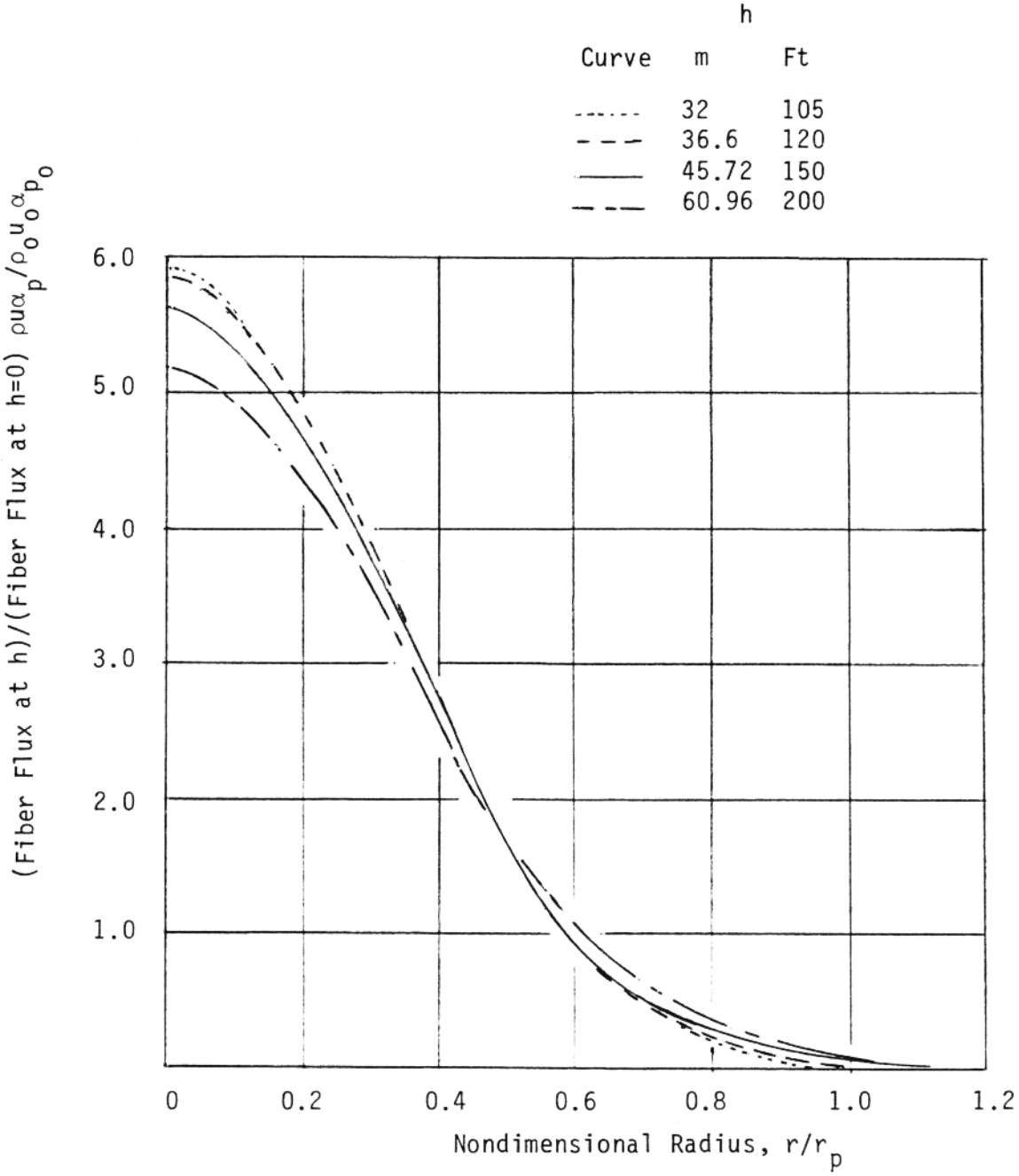

Figure 22. Normalized Fiber Flux Profiles as a Function of Height, 10.67 (35 foot) Diameter Fire

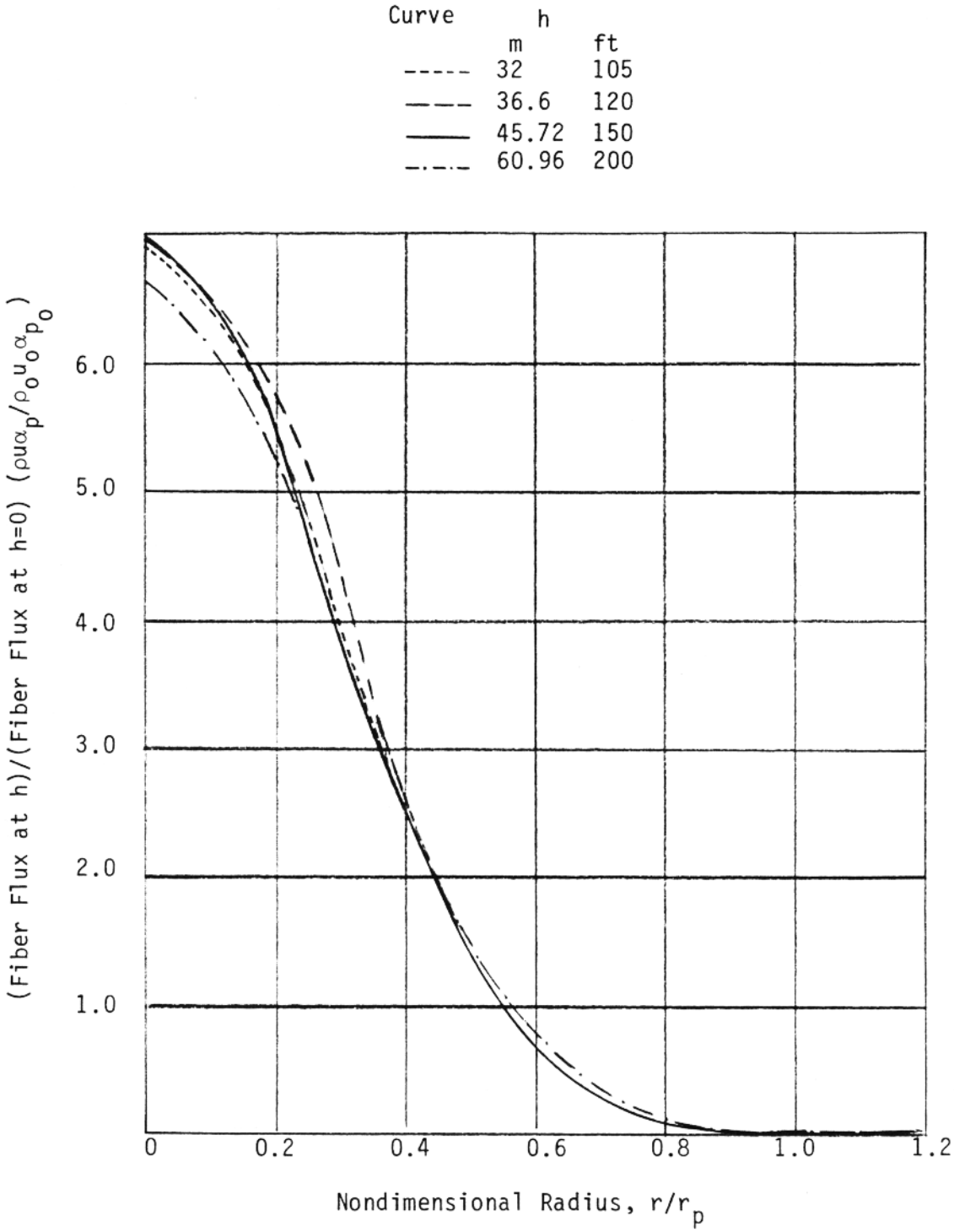

Figure 23. Normalized Fiber Flux Profiles as a Function of Height, 15 M (50 foot) diameter fire

In all cases, because of the tendency of the fire to "neck down," the large majority of fibers are observed, even at the 61 meter (200 foot) height, to be in a region within one pool radius of the centerline. In addition, this "necking down" tendency, as was reported in Ref. 1, leads to high-altitude ($\sim$ 100 ft or greater) fiber concentration profiles that are essentially independent of the initial location of the fibers within the fuel pool at h = 0; therefore, the results shown in Figures 21-23 can be used to estimate fiber fluxes for any arbitary (but axisymmetric) initial fiber distribution.

6. CONCLUSIONS AND RECOMMENDATIONS

Because the model modification effort detailed in this report is of a preliminary nature, the conclusions and recommendations reached should also be viewed as preliminary; subsequent work will lead to their refinement as well as further model refinement. However, a number of conclusions and recommendations can be drawn from this preliminary effort.

1. An analytical model of large pool fires which is in good agreement with measured fire structure data has been developed. This model can be used as a tool for the analysis and interpretation of large-scale fire measurements and consumption of fibers in a large scale fire.

2. Measured and computed temperature and species profiles show that significant unmixedness and incomplete combustion effects are present in large JP-4 pool fires.

3. Computational results indicate that the effects on fiber consumption of locally high temperatures because of temperature fluctuations in the fire are negligible; similarly the short residence time of the fibers in regions of the fire calculation in which mean temperature is overpredicted compared to the measurements indicates that the overprediction of temperature in these regions should not greatly affect the overall fiber consumption prediction. There is, however, a need for further verification of the fiber consumption rate expression over a range of oxygen concentrations typical of a fire.

4. While particle thermal nonequilibrium can result in some temperature mismatch between the fibers and gas phase, the overall effects of nonequilibrium

particle heat-up and cool-down tend to compensate resulting in only a small overall effect on particle consumption.

5. Based on the particle consumption expression defined in this report, overall single-fiber particle consumption of about 15% of the total particle mass is computed for large pool fires.

Preliminary recommendations can be itemized as follows:

1. Unmixedness effects in large fires need to be more thoroughly examined. In particular, the application of an unmixedness model to the fuel as well as the oxidizer, and the computation of unmixedness through a concentration fluctuation transport equation should be pursued.

2. The effects of the mixing and combustion process in the lower regions of the fire should be examined in more detail than is possible using a parabolic fire model.

3. Fiber consumption rates should be more thoroughly documented, including the possible effects of surface coatings.

7. REFERENCES

1. "Analytical Prediction of Atmospheric Plumes and Associated Particle Dispersal Generated by Large Open Fires, Task II Interim Technical Progress Report," Report SAI-78-009-WH, prepared for NASA Ames Research Center, Contract NAS2-10039, Science Applications, Inc., October 1978.

2. Boccio, J. L., Weilerstein, G., and Edelman, R. B., "A Mathematical Model for Jet Engine Combustor Pollutant Emissions," NASA-CR-121208, 1973.

3. Lee, K. B., Thring, M. W., and Beer, J. M., "On The Rate of Combustion of Soot in a Laminar Soot Flame," Combustion and Flame, Vol. 6, pp. 137-145, 1962.

4. Alpinieri, L. J., "Turbulent Mixing of Coaxial Jets," AIAA Journal, Vol. 2, No. 9, September 1964, pp. 1560-1567.